

Coarse sediment dynamics in a large glaciated river system: Holocene history and storage dynamics dictate contemporary climate sensitivity

Scott W. Anderson[†] and Kristin L. Jaeger

Washington Water Science Center, U.S. Geological Survey, Tacoma, Washington 98402, USA

ABSTRACT

The gravel-bedded White River drains a 1279 km² basin in Washington State, with lowlands sculpted by continental glaciation and headwaters on an actively glaciated stratovolcano. Chronic aggradation along an alluvial fan near the river's mouth has progressively reduced flood conveyance. In order to better understand how forecasted climate change may influence coarse sediment delivery and aggradation rates in this lowland depositional setting, we assessed the contemporary delivery and routing of coarse sediment through the watershed; this assessment was based on a rich set of topographic, sedimentologic, and hydrologic data from the past century, with a focus on repeat high-resolution topographic surveys from the past decade.

We found that most of the lower river's contemporary bed-load flux originates from persistent erosion of alluvial deposits in the lower watershed. This erosion is a response to a drop in local base level caused by a major avulsion across the fan in 1906 and then augmented by subsequent dredging. The 1906 avulsion and modern disequilibrium valley profiles reflect landscape conditioning by continental glaciation and a massive mid-Holocene lahar. In the proglacial headwaters, infrequent large sediment pulses have accomplished most of the observed coarse sediment export, with exported material blanketing downstream valley floors; during typical floods, transported bed material is largely sourced from erosion of these valley floor floods. Throughout the watershed, we observe decadal-scale coarse sediment dynamics strongly related to the filling or emptying of valley-scale sediment storage over 10²–10⁴ yr time scales, often in response to major disturbances that either

emplace large deposits or influence their redistribution. Paraglacial responses in large watersheds are suggested to be inherently complicated and punctuated as a result of internal landform interactions and stochastic/threshold-dependent events. We argue that, in combination, Holocene disturbance, storage dynamics, and human flow modification make coarse sediment fluxes in the lower White River relatively insensitive to decadal climate variability. Results highlight the degree to which river sensitivity to contemporary disturbance, climatic or otherwise, may be contingent on local and idiosyncratic watershed histories, underscoring the need to unpack those histories while demonstrating the utility of watershed-scale high-resolution topography toward that end.

INTRODUCTION

Changes in upstream sediment or water delivery or downstream changes in base level can trigger adjustments in alluvial river systems that propagate according to the dynamics of sediment transport (Schumm and Parker, 1973; James, 1991; Simpson and Castelltort, 2012; Pizzuto et al., 2017). An understanding of these propagating adjustments is fundamental to the interpretation of depositional stratigraphy, understanding causes and effects of historic geomorphic change, and forecasting channel responses to climate change or river engineering and restoration projects.

At watershed scales, much of the complexity of sediment dynamics can be linked to the intermittent storage and release of sediment from zones of transient storage, with rest periods ranging from years to millennia (Walling, 1983; Meade, 1988; Fryirs, 2013; Paola, 2016). Storage is tightly linked to the propagation or obscuring of sediment transport signals, given that any imbalance between upstream sediment input and downstream export must be accommodated by an equivalent storage change. Storage dynamics have been observed to play a large role in both the short- and long-term impacts of

increased sediment delivery; watersheds subjected to large increases in sediment delivery have tended to place large volumes of sediment into storage, mediating the short-term routing of material through the primary active channel; over the long-term, the re-entrainment of that stored material may influence river form and function long after the initial disturbance and short-term channel responses subside (Trimble, 1999; James, 1991, 2010; Madej and Ozaki, 2009). More generally, storage can effectively decouple downstream sediment loads from headwater sediment delivery over both management and geologic time scales (Church and Ryder, 1972; Dietrich and Dunne, 1978; Walling, 1983; Church and Slaymaker, 1989; Trimble, 1997, 1999; Simpson and Castelltort, 2012; Pizzuto et al., 2017).

In alpine watersheds, climate change over periods of decades to centuries represents one possible driver of changing upstream sediment delivery (O'Connor and Costa, 1993; Heckmann et al., 2016; Carrivick and Heckmann, 2017; Lane et al., 2017; Naylor et al., 2017). Recent changes in glacier area (e.g., Zemp et al., 2009), snowpack persistence, and hydrology (e.g., Stewart, 2009) in headwater settings have been well documented; whether these changes in headwater conditions are likely to result in downstream channel responses is less clear, and it depends both on the sensitivity of headwater sediment delivery to these short-term climatic changes and the degree to which changes in headwater sediment delivery are propagated downstream and persist as a significant perturbation to the downstream alluvial system (Brunsden and Thornes, 1979; Lisle, 2008; James, 2010; Bogen et al., 2015; Fryirs, 2017; Lane et al., 2017). In the context of potential changes in the form or mean elevation of downstream alluvial rivers, the delivery and transport of channel-forming coarse material are most directly relevant, and so was the focus of this study.

In western Washington State, sediment-rich rivers draining glaciated stratovolcanoes of the Cascade Range traverse the heavily populated Puget Lowlands before entering Puget

Scott Anderson  <http://orcid.org/http://orcid.org/0000-0003-1678-5204>
[†]swanderson@usgs.gov.

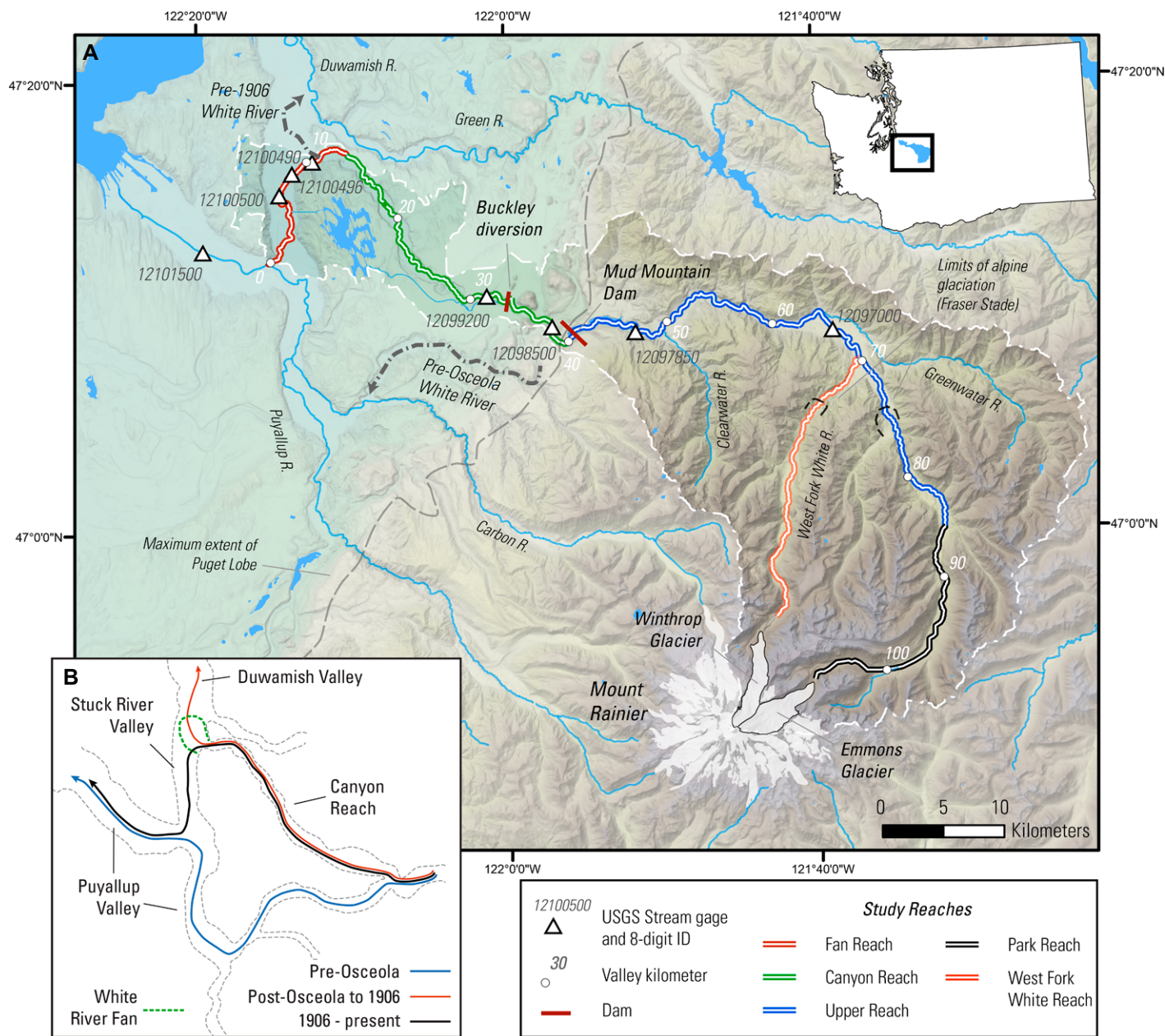


Figure 1. Overview map of White River watershed. (A) White River watershed and surrounding area. Maximum extents of the Puget Lobe and alpine glaciers during the Vashon Stade are delineated. R—River. (B) Simplified map of different routings of the lower White River over the Holocene. Light-green dashed line indicates approximate location of the White River fan. USGS—U.S. Geological Survey.

Sound (Fig. 1). Understanding the geomorphic evolution of these dynamic river systems is of practical importance for management of channel migration and flood risks, as well as preservation of regionally iconic and environmentally sensitive salmon populations. Correlations between sediment fluxes or channel form and regional climate suggest that sediment and channel processes in the region may be responsive to decadal-scale climate variability (Menounos and Clague, 2008; Czuba et al., 2012b; East et al., 2017; Anderson and

Konrad, 2019). However, the mechanisms and regional consistency of these linkages remain poorly understood. The Puget Lowlands are a low-relief landscape left behind after the retreat of the continental glaciers, and the paraglacial relaxation of regional rivers (Ballantyne, 2002a) is ongoing (Collins and Montgomery, 2011).

This study focused on the White River, which has its headwaters in glaciated terrain on the north flank of Mount Rainier (Fig. 1). Management concerns in the White River center on sedi-

ment delivery to a populated alluvial fan near the river's mouth, where chronic deposition over the past century has already substantially decreased flood conveyance (Dunne, 1986; Herrera Environmental Consultants, 2010).

The motivation for this study was to provide guidance on how forecasted changes in regional climate may influence coarse sediment delivery to the White River fan; since the alluvial fan traps essentially all incoming coarse sediment, any change in coarse sediment flux, climate-driven or otherwise, would be expected to have a direct

impact on deposition rates. While the motivation here is specific and applied, the underlying question of how external signals propagate and manifest in depositional settings is a central theme in fluvial geomorphology.

Since these questions are inherently related to the watershed-scale delivery and routing of coarse sediment, we approached this problem by attempting to improve our understanding of those coarse sediment dynamics in the White River. To this end, we made use of a large set of repeat high-resolution topographic surveys covering the major river valleys and proglacial areas, supplemented by hydrologic, older topographic, and sediment transport data sets. We also drew heavily on prior geologic studies of the late Quaternary history of the White River; the watershed was extensively reworked by continental and alpine glaciers during the Last Glacial Maximum, and by major lahars from Mount Rainier in the millennia since. As our results bear out, this history of disturbance and the associated storage dynamics are central factors in understanding the contemporary processes in the White River, including its likely sensitivity to climate.

SETTING

Locations along the White River are given as kilometers upstream from its confluence with the Puyallup River, measured along the valley centerline (valley kilometers, or Vkm). The White River was broken up into four study reaches with similar physiographic characteristics (Figs. 1 and 2). The West Fork White River, as a key sediment-rich tributary, constituted a fifth study reach. Locations along the West Fork White River are notated as WF-Vkm, starting with WF-Vkm 70 at the confluence with the White River and increasing upstream.

Geology, Hydrology, and Channel Morphology of the White River

The White River drains a 1279 km² basin with headwaters on the north flank of Mount Rainier (4392 m) in Washington State (Figs. 1 and 2). Mount Rainier and surrounding headwaters are located within the federally designated Mount Rainier National Park. The White River emerges from the terminus of Emmons Glacier and then flows 105 km before joining the Puyallup River and emptying into central Puget Sound. Major tributaries to the White River include the West Fork White River, which emanates from Winthrop Glacier on Mount Rainier, and the unglaciated Greenwater and Clearwater Rivers. The White River Basin is located within a rain-snow mixed-precipitation

regime. The largest-magnitude floods occur in fall and winter, associated with warm rain or rain-on-snow events often referred to as atmospheric rivers (Neiman et al., 2011; Konrad and Dettinger, 2017). Smaller peaks occur in the spring in association with snowmelt runoff (Fig. S1¹).

Mount Rainier is a heavily glaciated stratovolcano composed of stratified andesite and dacite lavas (Driedger and Kennard, 1986; Reid et al., 2001). The mountainous terrain surrounding Mount Rainier is formed of a complex assemblage of tertiary intrusive and extrusive volcanic rocks. During the Last Glacial Maximum, the Puget Lobe of the Cordilleran ice sheet covered the lower watershed to the limits of the contemporary mountain front (Fig. 1; Booth et al., 2003). The subsequent retreat between 16 and 15 k.y. B.P. left behind a landscape of low-gradient glacial, glacio-fluvial, and glacio-lacustrine deposits and deep glacial troughs, the latter of which became the inland waterways of Puget Sound. Concurrent alpine glaciation during the Fraser Stade extended down the White River valley to Vkm 75 and down the West Fork White River to WF-Vkm 75 (Fig. 1), and alpine glaciers likely formed a full ice cap over much of the upper watershed in prior stades (Crandell and Miller, 1974). However, glacial valley fills have largely been covered by volcanoclastic material in the upper White River and West Fork White River valleys, most notably from the 5600-yr-old Osceola Mudflow (Crandell, 1971; Crandell and Miller, 1974).

The White River is predominately alluvial, with bed material composed of sand, gravel, and cobbles. Subsurface grain-size distributions are relatively consistent down the length of the basin, with median diameters of ~30–50 mm (Fig. S2; see supplementary text [footnote 1] for data collection methods). As a result of the combined effects of glacial and postglacial processes, the White River flows through a regionally consistent sequence of distinct reaches (Collins and Montgomery, 2011) that include mountain valley headwaters (park and upper reaches), a short, steep bedrock canyon (the divide between the upper and canyon reaches), a postglacial valley, in which rivers have incised through continental glacial deposits (canyon reach), and a low-gradient glacial valley, where glacial troughs have been progressively filled by postglacial deposition (fan reach).

¹Supplemental Material. Description of ancillary data collection methods and supporting figures. Please visit <https://doi.org/10.1130/GSAB.S.12616562> to access the supplemental material, and contact editing@geosociety.org with any questions.

Osceola Mudflow

The White, Puyallup, and the north-neighboring Duwamish River systems (Fig. 1) were substantially modified by the Osceola Mudflow, a 5600-yr-old, 3.8 km³ lahar originating on the northeast flank of Mount Rainier (Crandell, 1971; Mullineaux, 1974; Dragovich et al., 1994; Vallance and Scott, 1997). Prior to that event, the White River turned south near the mountain front (~Vkm 40), connecting to the Puyallup River via the Carbon River (Fig. 1). The Osceola Mudflow choked that southern route, causing the river to avulse and flow over a broad plain of glacial drift to the northwest and ultimately fall into a north-south-trending embayment that now forms the modern Duwamish and Stuck River valleys. The canyon reach of the White River was formed as the river incised through that glacial drift, while sediment deposited in the downstream north-south-trending embayment formed the White River fan. Most of the substantial sediment load that transited the White River fan was routed to the north, filling the Duwamish embayment to create the modern Duwamish River valley (Fig. 1B; Dragovich et al., 1994).

1906 Avulsion and Historic Channel and Flow Modifications

The White River watershed changed substantially again over the twentieth century, due to both natural and human influences. During European settlement of the area in the nineteenth century, the White River turned north where it exited the canyon reach, exiting into Puget Sound near Seattle (Fig. 1). The valley linking the White River to the Puyallup River was then occupied by the Stuck River, a small distributary of the White River (Ober, 1898). Examinations of valley-floor geometry and surficial deposits in 1907 indicated that the northern Duwamish route had been the primary course of the lower White River for at least several hundred years prior (Chittenden, 1907).

In 1906, the White River breached a low divide separating the White and Stuck Rivers, resulting in an avulsion of the White River into the Stuck River valley and down to the Puyallup River (Fig. 1B). This disruptive event motivated a substantial multicounty management response to deal with the new course of the White River and the enlarged Puyallup River; major management activities over the following decades included the permanent closure of the pre-avulsion river path by a concrete structure near Vkm 11, straightening of the lower Puyallup River, and dredging of the new alignment of the lower White River. Construction of bank protection

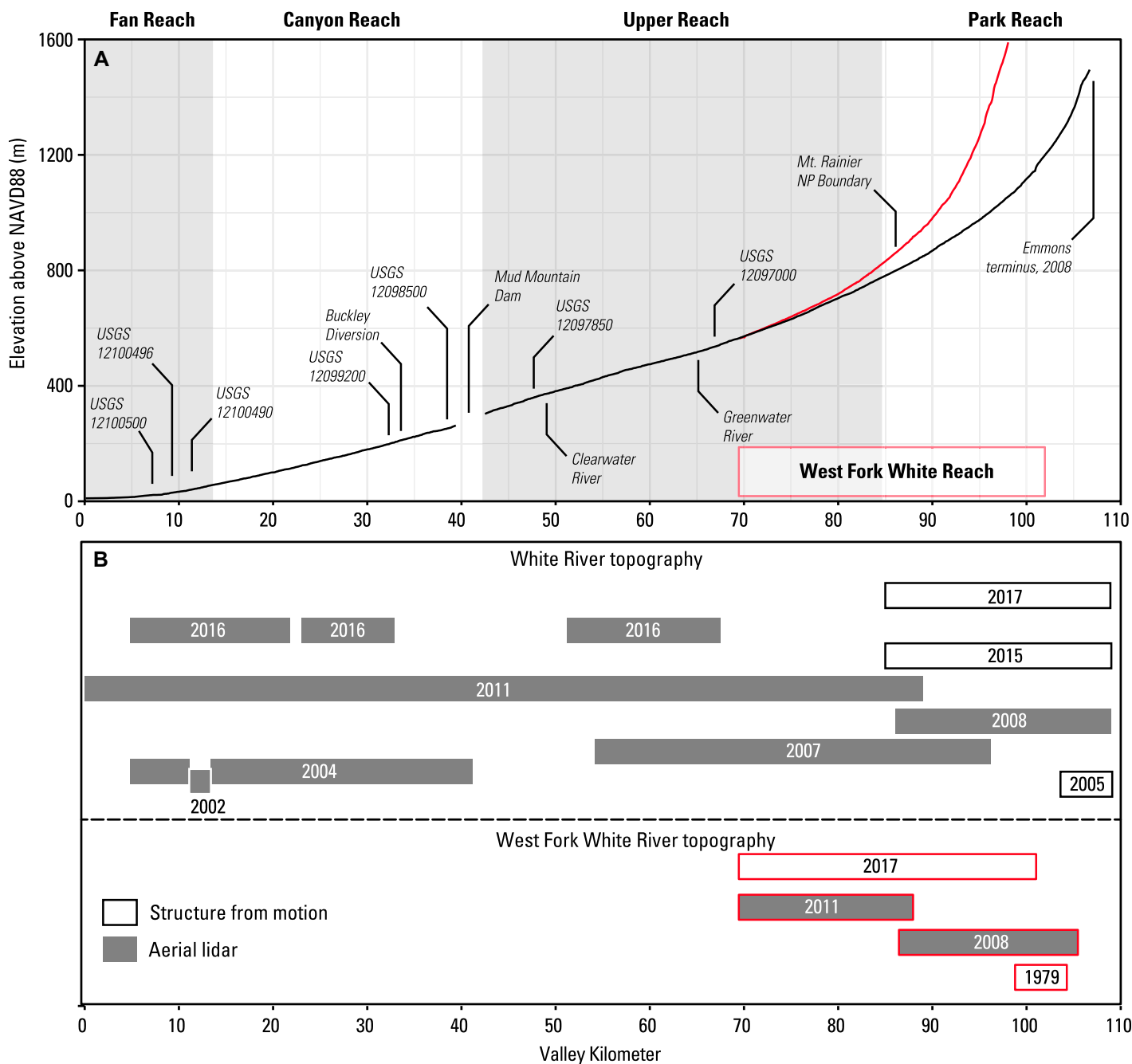


Figure 2. Longitudinal profile of White and West Fork White Rivers and extents of high-resolution topographic surveys. (A) Longitudinal profiles of water surface elevation, based on 2008 and 2011 light detection and ranging (LiDAR) data, along with reach divisions and locations of gages, major tributary confluences, and dams. USGS—U.S. Geological Survey; NP—National Park; NAVD88—North American Vertical Datum of 1988. (B) Longitudinal extent and collection year for topographic surveys.

structures and levees and clearing of woody debris occurred throughout both the White and lower Puyallup Rivers.

Following damaging floods in the 1920s and 1930s, Mud Mountain Dam was constructed in a narrow bedrock canyon near Vkm 40. The dam was used to desynchronize and so reduce flood peaks on the Puyallup River while also providing direct flood protection on the White River.

The dam typically holds little to no pool over most of the year and is filled only during floods. Stored water is typically released within several days to weeks through tunnels with invert elevations near the predam river bed, allowing most of the accumulated silt and sand, and some fraction of the gravel, to continue moving downstream (Dunne, 1986). Starting in 2009, aggradation and loss of flood conveyance in the fan reach

caused the U.S. Army Corps of Engineers to reduce maximum outflows from the dam to 200 m³/s, down from the pre-2009 limit of 340 m³/s (Fig. 3B).

Water and sediment fluxes in the lower White River have also been modified by a low-head diversion dam near Vkm 33, constructed in 1911 for hydroelectric power generation from Lake Tapps. The 3.5-m-high dam was constructed

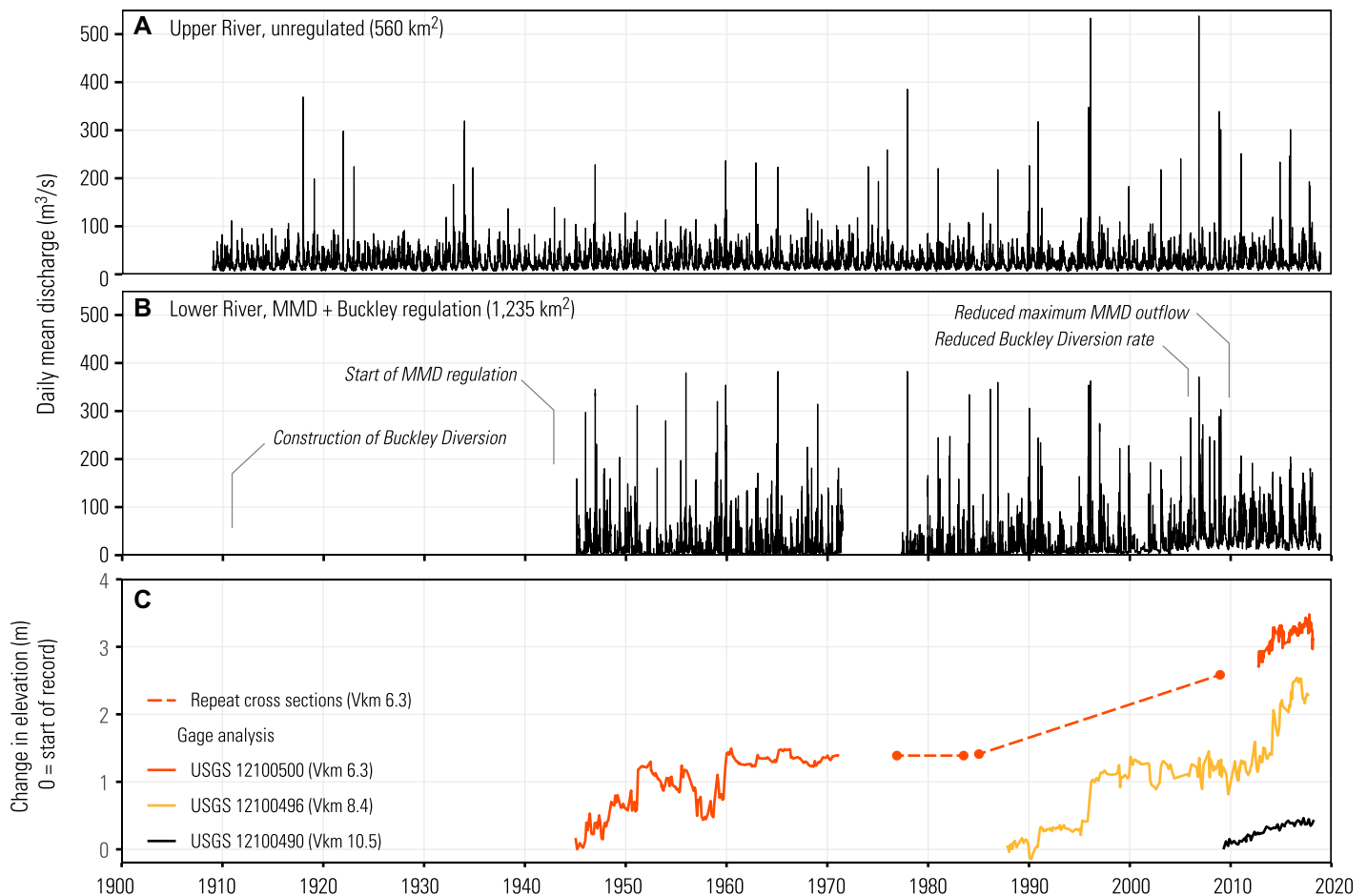


Figure 3. Long-term discharge records and lower-river aggradation trends. (A) Daily mean discharge records for the unregulated upper river at U.S. Geological Survey (USGS) gage 12097000. (B) Daily mean discharge records for the lower river at USGS gage 12100500, in the regulated fan reach. Methods used to extend available gage records to the long-term records shown here are described in the Supplemental Material (see text footnote 1). MMD—Mud Mountain Dam. (C) Aggradation trends in the fan reach, based on changing stage-discharge relations at USGS gages and repeat cross sections collocated with gage sites; Vkm—valley kilometer (Prych, 1988; Czuba et al., 2010).

with 2-m-high wooden flashboards that purposely fail during floods, reducing the diversion of water and sediment and allowing some of the sediment accumulated upstream to pass (Cooper, 1983). Prior to 2005, the structure typically diverted ~60% of the total annual discharge, presumably carrying relatively large volumes of silt and sand plus an unknown fraction of the river's bed load; since 2005, water diversions, and so presumably sediment diversion, have been reduced to negligible levels (Fig. 3B).

Prior Studies of Downstream Aggradation, Sediment Sourcing, and Transport Rates

Deposition of sand and gravel in the fan reach has been a chronic and well-documented issue (Dunne, 1986; Prych, 1988; Sikonia, 1990; Herrera Environmental Consultants, 2010; Czuba et al., 2010, 2012a), and multiple lines of evidence indicate that the White River fan traps

essentially all delivered bed load (Czuba et al., 2012a). Regular dredging had historically been used to maintain flood conveyance through this reach, but this practice ceased in the 1980s. Since the late 1980s, the lower river has aggraded about 2 m, averaging ~0.05 m/yr (Herrera Environmental Consultants, 2010). Long-term gage records suggest an overall net aggradation of about 3 m in this reach since 1945 (Fig. 3C).

Concerns about aggradation in the fan reach have motivated watershed-scale assessments of the coarse sediment dynamics in the White River by Dunne (1986) and, as part of a larger study of the Puyallup watershed, by Czuba et al. (2010, 2012a). Dunne (1986) cited the poorly sorted character of bed material and the geologic context of the Osceola Mudflow to argue that most of the gravel load in the lower river was likely a result of erosion of the canyon reach, even if most of the suspended load came from the upper glaciated watershed. Czuba et al. (2010,

2012a) presented a wide range of analyses that focused on Mount Rainier as a significant source of both suspended-load and bed-load material to the lower reaches of the White and Puyallup River systems.

Previous studies have estimated sediment fluxes in White River based on direct measurements of either suspended-load or bed-load flux and the development of discharge-flux or turbidity-concentration rating curves. Over water years 2011–2018, estimated suspended sediment loads in the upper watershed (immediately upstream of Mud Mountain Dam; Nelson, 1979) were $630,000 \pm 100,000$ tonnes/yr, while suspended sediment loads in the lower watershed (at the upstream extent of the fan reach; Czuba et al., 2012a) averaged $560,000 \pm 160,000$ tonnes/yr (here and throughout, uncertainty bounds around rating-curve-derived fluxes represent 95% confidence intervals, estimated based on regression uncertainty using methods presented

in Gilroy et al. [1990]). The suspended load at both sites was composed of 60% sand and 40% silt and clay. Though there is substantial uncertainty when comparing rating curves developed in different eras (Warrick, 2015), the general similarity in the magnitude and grain size of these estimates supports the notion that most of the lower-river suspended silt, sand, and clay originates from the watershed upstream of Mud Mountain Dam, and that Mud Mountain Dam does not persistently trap much of the suspended sediment load. This latter point is independently corroborated by the lack of measured sediment accumulation behind Mud Mountain Dam (Dunne, 1986).

Estimated annual bed-load flux in the upper fan reach was $26,000 \pm 11,000$ tonnes/yr from 2011 to 2018, equivalent to a volume of $16,000 \pm 6,500$ m³/yr (here and throughout, relations between mass and volume for bed load and bed material were based on a bulk density of 1.6 tonnes/m³), composed of 50% sand and 50% gravel (Czuba et al., 2012a). A measurement-based bed-load rating curve developed above Mud Mountain Dam nominally produces a similar estimate of the mean annual bed-load flux (Nelson, 1979). However, the 1970s upper-watershed measurements were primarily composed of sand, which typically moves in suspension (Fig. S2). A reanalysis of these measurements, truncated to only include material coarser than 0.5 mm, indicates a 2011–2018 mean annual bed material flux of 7500 ± 1500 m³/yr. Given the age and questionable accuracy of these upper-watershed bed-load measurements, however, true uncertainty is likely larger than regression strength alone would indicate.

Historic and Forecasted Regional Climate Change

Over the period of the observational record, mean annual temperatures in Puget Sound show a long-term increasing trend, while annual precipitation has shown no long-term trend (Mauger et al., 2015). Decadal variability in conditions in the North Pacific Ocean, characterized in indices such as the Pacific Decadal Oscillation or the North Pacific Index, drives similar decadal variability in regional climate and climate-impacted processes (Mantua and Hare, 2002; Whitfield et al., 2010).

Glaciers on Mount Rainier have generally been retreating since the mid-nineteenth century, though rapid retreat from 1920 to 1945 and from 1980 to the present was separated by a period of re-advance from 1950 to 1980 (Nylen, 2004); similar trends are seen throughout the region (i.e., Dick, 2013). Peak seasonal snowpack accumulations have shown multidecadal variability

with a weak overall negative trend since 1930 (Stoelinga et al., 2010). Secular trends in annual maximum precipitation and river discharge in rainfall-dominated flood systems, such as the White River, tend to be positive in the region, though trends are typically small in comparison to variability (Fig. 3A; see supplementary text for methods used to compile long-term hydrologic records; Mass et al., 2011; Mastin et al., 2016).

Over the next 50–100 yr, regional climate models project with good confidence continued increases in temperature, loss of glacier area, and increased probabilities of precipitation falling as rain (Hamlet et al., 2013; Frans, 2015). The magnitudes of the largest rain and flood events are forecasted to increase, though uncertainty in these forecasts is large (Salathé et al., 2014; Tohver et al., 2014; Warner et al., 2015). Total precipitation is not forecasted to change markedly.

Study Approach

The goal of this study was to better understand the controls on coarse sediment delivery to the White River fan over multi-decadal timescales. We approached this problem using historic observational information about geomorphic change and sediment fluxes over the past century, with a focus on the data-rich last several decades, to better understand contemporary coarse sediment sources, sinks, and connectivity at the watershed scale. Results were interpreted against the backdrop of the White River's known history of glacial, volcanic, and human disturbance.

This study was particularly motivated by questions of whether forecasted changes in climate are likely to increase coarse sediment delivery to the lower river; we specifically considered two potential pathways of impact. First, loss of glacier and snow cover, coupled with increases in storm magnitude or frequency, may increase sediment delivery from headwaters on Mount Rainier. If such a signal is both generated and propagated through the watershed, sediment delivery to the fan reach for a given flood magnitude may increase. Second, increasing frequencies or magnitudes of floods may increase sediment fluxes throughout the watershed, regardless of whether sediment concentrations change during a given flood.

The primary tool used in this study was the differencing of high-resolution topographic surveys; each of the major study reaches has topographic coverage in three digital elevation models (DEMs), providing two periods of topographic change. These analyses were supplemented by analyses of repeat cross section surveys through the Mud Mountain Dam impoundment area,

geomorphic analysis of stream gage data, direct measurements of sediment flux, and a unique set of detailed surveys of the lower White River from 1907. We focused on the delivery and transport of bed material. We use “bed material” and “coarse sediment” interchangeably throughout this article. Results are presented in a sequence of vignettes, one for each of the major study reaches plus one for Mud Mountain Dam, presented in upstream to downstream order. These reach-scale results were then used to provide an integrated view of contemporary coarse sediment dynamics in the White River.

METHODS

High-Resolution Topographic Differencing

Differencing of high-resolution topographic surveys was used to assess changes in sediment storage and sediment transfer along the length of the White River valley floor and in proglacial basins. In total, 11 high-resolution (0.5–2 m) rasterized DEMs were used in this study and differenced to create DEMs of difference (DoDs; Fig. 2; Table 1). Six of these DEMs were derived from aerial light detection and ranging (LiDAR) data publicly available through the Puget Sound Lidar Consortium (Table 1). The remaining five DEMs were derived using Structure-from-Motion (SfM) photogrammetry acquired as part of this study. Collection of source imagery, ground control, and processing for 2015 and 2017 SfM surveys, which covered the proglacial zones of the Emmons and Winthrop Glaciers and the upstream-most 20 km of the White and West Fork White Rivers, followed methods described in Anderson et al. (2017). Ground control for preexisting imagery, which included photos of the Emmons proglacial area from 2005 and the Winthrop proglacial area from 1979, was derived from 2008 aerial LiDAR intensity images, but was otherwise processed in the same fashion as the new imagery collections. More details about the SfM products are available in Anderson and Jaeger (2019).

In two instances, DEMs from different years were combined to provide complete spatial coverage in a reach. In the fan reach, data from a 2002 LiDAR survey were used to fill a 2 km gap in the 2004 data (Fig. 2). In the West Fork White River, LiDAR data from 2008 and 2011 were used in combination to provide a spatially continuous baseline against which to compare 2017 topography.

Various coregistration methods were used to reduce highly correlated or systematic errors, which tended to dominate the total error budget (Anderson, 2019). Outside of the proglacial basins, measured change along road surfaces

TABLE 1. DATA SETS USED IN STUDY

Date or date range	Spatial extent	Repository	Note
<u>Lidar DEMs*—All PSLC data available at: https://pugetsoundlidar.ess.washington.edu/</u>			
2002	Vkm 11.1–13.4	PSLC	
2004	Vkm 4.8–11.1, 13.4–41.2	PSLC	2004 bare-earth DEM derived from classified point cloud data on repository
2007	Vkm 54.2–96.2	PSLC	
2008	Vkm 86.1–110.0; WF-Vkm 87.0–105.0	PSLC	
2011	Vkm 0.0–89.0; WF-Vkm 70.0–87.5	PSLC	2011 bare-earth DEM derived from classified point cloud data on repository
2016	Vkm 4.8–21.8; 23.0–32.9; 51.2–67.5	PSLC	Coverage includes overflight data acquired directly from vendor for this study
<u>Structure-from-Motion DEMs—For data in ScienceBase repository, see Anderson and Jaeger (2019; https://doi.org/10.5066/P9HT46KB)</u>			
1979	WF-Vkm 93.0–105.0	ScienceBase	Original imagery from Nolan et al. (2017).
2005	Vkm 105.5–110.0	ScienceBase	Original imagery scanned from negatives provided by National Park Service.
2015	Vkm 85.0–110.0	ScienceBase	
2017	Vkm 85.0–110.0; WF-Vkm 70.0–103.0	ScienceBase	
<u>Aerial imagery</u>			
1940	Vkm 0.0–40.0	UW-RHP	http://riverhistory.ess.washington.edu/
2009	Entire watershed	NAIP	
<u>Historic channel maps</u>			
1907	Vkm 0.0–16.0	ScienceBase	
<u>USGS Stream gauge data</u>			
Various	Various	NWIS	Includes all discharge records, MMD pool elevations, and streamflow measurement data.
<u>Mud Mountain Dam cross sections</u>			
1951–2011	Vkm 40.5–47.8	U.S. Army Corps of Engineers	Contact Zac Corum (Zachary.P.Corum@usace.army.mil) for data.
<u>Bed material grain-size distributions</u>			
2018	Vkm 11.0–89.0	ScienceBase	
<u>Bed-load samples</u>			
1974–1976	Vkm 46.8	NWIS; Nelson (1979)	
2010–2011	Vkm 10.5	NWIS; Czuba et al. (2012a)	

Note: LiDAR—light detection and ranging; DEM—digital elevation model; MMD—Mud Mountain Dam; NAIP—National Agriculture Inventory Program; NWIS—National Water Information System; NPS—National Park Service; PSLC—Puget Sound LiDAR consortium; UW-RHP—University of Washington River History Project; Vkm—valley kilometer; WF-Vkm—West Fork White River valley kilometer; USGS—U.S. Geological Survey.

*Year for LiDAR is given as year in which majority of data were collected if collection spanned multiple calendar years.

(fan, canyon, and upper reaches) or stable, bare-gravel surfaces (park, west fork reaches) was used to estimate and correct 0.05–0.50 m vertical registration offsets between data sets. The vertical correction was allowed to vary continuously along the length of the valleys. In the proglacial basins, both vertical and horizontal offsets were corrected based on systematic relations among slope, aspect, and measured change on stable, unvegetated hillslopes (Nuth and Kääh, 2011). Nonlinear “doming” errors in proglacial SfM data sets (James and Robson, 2014) were further reduced by interpolating and subtracting a continuously varying error surface fit to measured change in stable parts of the landscape using a kernel-based interpolation scheme.

Differences in discharge at the time of the different LiDAR surveys resulted in measured volumetric change as a result of the different volumes of water held in the channel, creating an effective systematic error if results were interpreted in terms of sediment storage alone. To isolate volumetric change related to sediment storage, we used cross-sectional hydraulic relations to effectively “raise” the water surface in the lower-discharge survey to the level we would expect if the discharge had been higher. This involved two steps: (1) Channel width and local water surface slope were extracted at a cross section from the lower-flow LiDAR survey, and Manning’s equation was iteratively applied to estimate the thal-

weg depth for a simple triangular cross section that passed the known discharge. (2) That cross section was then extended using bank geometry extracted from the LiDAR data, and Manning’s equation was again used to iteratively raise the water surface until the estimated discharge matched that of the higher-discharge survey. A Manning’s n value of 0.04 was used throughout; different values of n primarily resulted in different estimates of thalweg depth, but they only weakly influenced estimates of modeled changes in water surface elevation.

This process was repeated at 100–200 m intervals and used to interpolate a continuous rasterized estimate of water surface elevation at the higher discharge. Points in the lower-discharge raster falling below this elevation were replaced with the estimated water surface elevation. This process was only applied in the fan, canyon, and upper reaches, since differences in river stage in the braided park and West Fork White River reaches represented a negligible fraction of total geomorphic change.

After correcting surveys to a common effective discharge, and assuming there were no substantial changes in reach-scale depth-discharge relations between surveys, the effective volume of water held in a given reach should be the same in both surveys. Any measured volumetric change between surveys should then primarily reflect changes in sediment storage, including

storage changes occurring in areas that were submerged in one or both surveys. Estimates of volumetric change using these discharge-corrected DEMs were then considered to be relatively complete estimates of storage change across the entire active channel.

Longitudinal patterns of gross erosion, deposition, and net change were quantified using regular valley-spanning polygons covering 250 m (park and West Fork reaches) or 500 m (fan, canyon, and upper reaches) swaths of the valley floor, measured along the valley centerline. To reduce the influence of residual systematic errors, the area of analysis was truncated to exclude broad areas of the valley floor where both measured change and geomorphic position suggested no true change had occurred. Estimates of gross erosion and deposition are based on thresholded DoDs (i.e. Wheaton et al., 2010), while estimates of net change were based on unthresholded DoDs (Anderson, 2019). A threshold value of 0.25 m was selected as typical of 2σ ranges for random errors across the various data sets.

Spatial patterns in sediment storage were visualized as the cumulative sum of net change, starting at the upstream edge of the DoD extent and moving downstream (“downstream cumulative net change”). Reaches of net erosion appear as a downward-trending line, while net depositional reaches appeared as upward-trending lines. The slope of the line provided a measure of the rate

of storage change (m^3/km), and the vertical difference between any two points on the line indicates the net change over the intervening reach.

Estimating Uncertainty in Topographic Change

Uncertainties in reach-scale net change were estimated by comparing, for a given reach, the sum of results from the two sub-intervals (i.e. $(\text{DEM}_3 - \text{DEM}_2) + (\text{DEM}_2 - \text{DEM}_1)$) against direct differencing of the first and last DEMs (i.e. $\text{DEM}_3 - \text{DEM}_1$); note that this more a measure of coregistration consistency than absolute accuracy. Coregistration and delineation of the geomorphically active areas were done independently for each of the three possible analysis intervals in a given reach. Differences in the mean vertical change estimates using the direct and sum-of-steps analyses were -0.029 , -0.041 , and 0.007 m in the canyon, upper, and park reaches, respectively. A uniform uncertainty of ± 0.05 m, interpreted as the 95% confidence interval (CI), was then used to calculate volumetric uncertainty bounds. This estimate represents the potential mean error over long reaches and is not an indication of point-level precision. Uncertainty in the proglacial areas was modeled as a spatially correlated error, with a 95% CI range of ± 0.4 m and a correlation range of 300 m, and propagated according to methods presented in Rolstad et al. (2009).

Relating Channel Change and Bed Material Flux

Mass balancing implies that changes in channel storage are inversely related to changes in bed material fluxes, and this is quantitatively described here using a simplified one-dimensional expression of the continuity equation,

$$\Delta V = Q_{S,in} - Q_{S,out},$$

where ΔV is the net volumetric change in a reach, and $Q_{S,in}$ and $Q_{S,out}$ represent the sediment fluxes at the upstream and downstream edges of that reach, respectively (Exner, 1925; Paola and Voller, 2005). If the absolute flux of bed material can be quantified at any point within a DoD, either through direct measurement or by identifying a location where the flux is presumed to be zero, continuity of mass can be used to estimate the absolute flux at any other point in the DoD (Lane et al., 1995).

1907 Channel Surveys

Chittenden's (1907) report following the 1906 White River avulsion included detailed surveys of the lower Puyallup River and the pre- and

postavulsion channels of the White River. These surveys included regular channel cross sections, water surface elevations, and high-water marks from the 1906 flood. These surveys captured the condition of the White River immediately after the 1906 avulsion but prior to the significant human modification that followed.

Scanned survey sheets were georeferenced using township and range corners and road or railroad alignments. A consistent offset between modern LiDAR elevations and 1907 survey points in stable, flat parts of the (off-channel) valley floor was used to reduce the 1907 elevations to modern North American Vertical Datum of 1988 (NAVD88) elevations, and this was independently corroborated by comparisons with stage-discharge changes in the lower Puyallup River. Channel position and elevations of the low-flow water surface and thalweg were digitized and compared against 2011 LiDAR water surface elevations to assess profile changes over the past century.

Mud Mountain Dam Cross Sections

Repeat cross sections in the Mud Mountain Dam impoundment, collected from 1951 to 2011, were supplied by the U.S. Army Corps of Engineers (USACE). Because of inconsistencies in data collection frequency or methods, a complete record of comparable cross sections was only available from 1960 to 2011, and it only covered over the lower half of the impoundment area (Fig. S3; see footnote 1).

Surveys collected from 1960 to 1993 all referenced the same concrete benchmarks set at cross-section ends, and so they share a common vertical datum. That datum is nominally referenced to the National Geodetic Vertical Datum of 1929 (NGVD29). The most recent 2011 survey was based on newly established controls referencing NAVD88, based on survey-grade global navigation satellite system (GNSS) occupations. After first converting 1993 data to NAVD88 elevations and subsetting points to those collected on moderate slopes above 350 m elevation (above the height of most impoundment pools and so unlikely to have experienced sediment accumulation), a persistent offset of 0.8 m was identified between the 1993 elevations and 2011 LiDAR elevation. This offset is presumed to have arisen from imperfect establishment of absolute elevations on the original concrete benchmarks used in pre-2011 surveys. This offset was then applied to all surveys collected on or before 1993 to bring them into proper alignment with NAVD88 elevations.

To isolate changes in coarse sediment storage from the fine sediment that tends to accumulate higher along the valley walls, cross sections

were truncated to include only the lateral widths of the active channel and adjacent low surfaces. Changes in cross-section area were calculated over those truncated lateral extents. Volumetric change over the lower half of the impoundment pool valley floor was then calculated by multiplying the length between sequential cross sections by the average area-change in those bounding cross sections (end-area averaging).

Geomorphic Analysis of Stream Gage Records

Streamflow measurements made in support of stream gauging provide long-term records of channel adjustments with monthly resolution (James, 1991; Slater et al., 2015; Anderson and Konrad, 2019; Pfeiffer et al., 2019). Changing channel conditions were assessed based on changes in stage-discharge relations and the Froude number, $Fr = U/(gD)^{0.5}$, where U is the mean velocity, D is the mean depth, and g is the acceleration of gravity. Changes in stage-discharge relations were interpreted primarily as a measure of changing channel elevation at the hydraulic control for the gage site (Anderson and Konrad, 2019). Changes in Froude number were interpreted as a measure of changing channel roughness, with lower Froude numbers implying a relatively rougher, more armored bed state, and higher Froude numbers implying smoother bed conditions with more abundant mobile material (i.e., Ritchie et al., 2018).

Changes in stage discharge and Froude number were both assessed by defining their average relation with discharge, fit using a LOESS curve (Cleveland and Devlin, 1988), and then assessing stage or Froude residuals relative to that relation over time (James, 1991; Slater et al., 2015). This analysis was limited to measurements made below the 75th percentile daily mean flow, and so it excluded high-flow measurements, which tend to show more random variability. For Froude number, the residual for a given measurement was added to the LOESS-fit Froude number at 40 m^3/s , which is roughly the mean annual flow at all relevant gages, so that corrected Froude numbers retained a physically meaningful range from zero to one.

RESULTS

Winthrop Proglacial Zone and West Fork White River

Since 1979, geomorphic activity in the Winthrop proglacial area has been dominated by extensive erosion during a massive storm that occurred in 2006 (Fig. 4; for details of the 2006 storm, see Legg et al., 2014). Erosion primarily

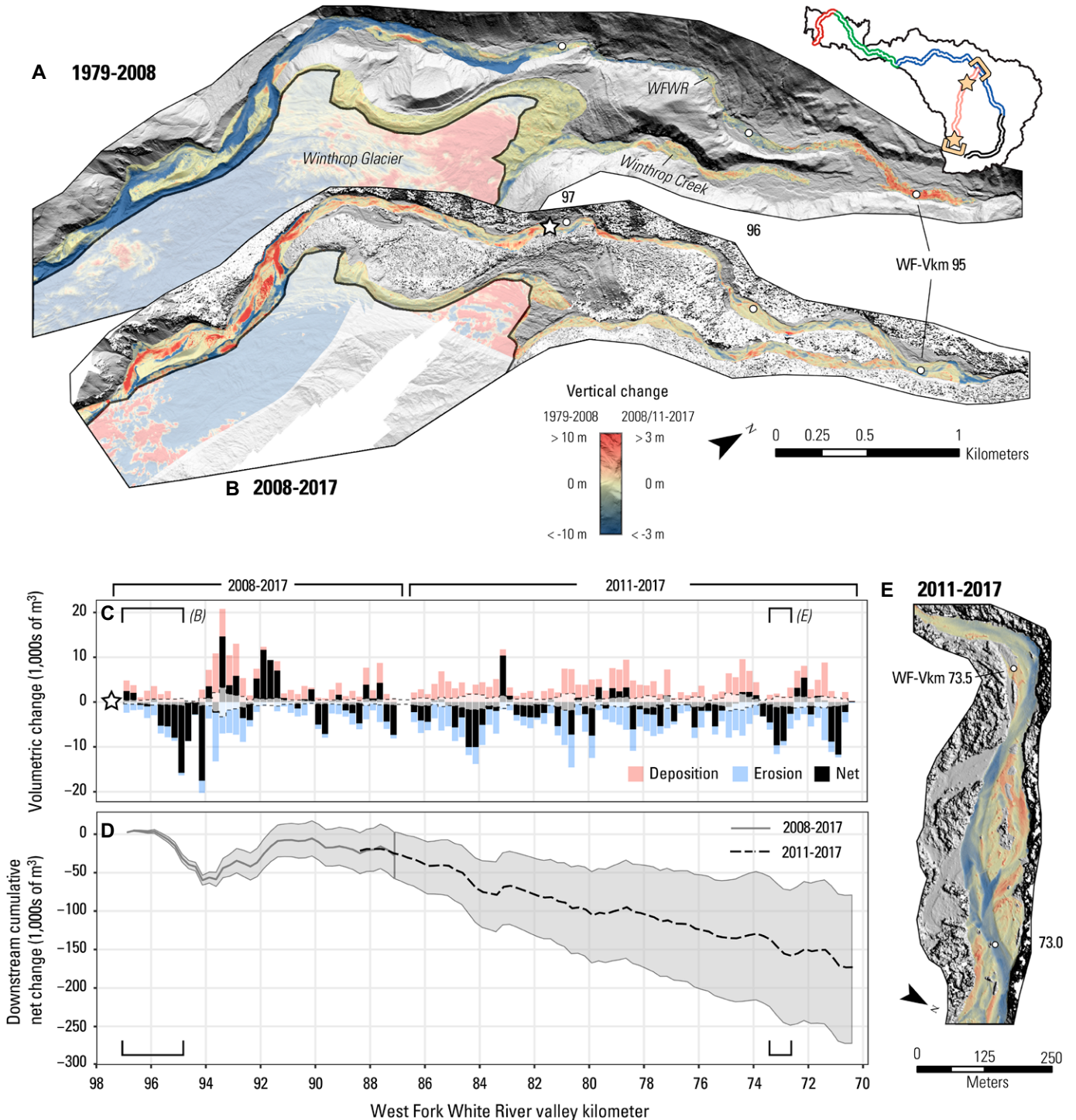


Figure 4. Topographic change in the Winthrop proglacial area and downstream West Fork White River (WFWR). (A–B) Digital elevation model (DEM) of difference showing elevation change in the Winthrop proglacial area and uppermost extents of the West Fork White River from 1979 to 2008 (A) and from 2008 to 2017 (B). Star at WFW-Vkm 97 in B indicates start of fluviially dominated geomorphic change presented in part C; geomorphic change upstream of that point is summarized in Table 2. Shaded areas indicate extent of the Winthrop Glacier. Note that range of vertical change indicated by color scale in A is substantially larger than for B or E, due to the exceptional magnitude of change that occurred over the 1979–2008 interval. (C) Gross deposition, gross erosion, and net change in sequential 250 m sections of the West Fork White River from 2008/2011–2017. Gray dashed lines indicate limits of detection (95% confidence intervals). (D) Downstream cumulative net change and 95% confidence intervals. Brackets in C and D indicate the location of change shown in B and E. (E) Example DEM of difference from the West Fork White River. Flow is from top to bottom. Inset in upper right of figure indicates extent of analysis relative to entire watershed (brackets) and specific locations of A/B and E (stars). Vkm—valley kilometer.

TABLE 2. VOLUMETRIC CHANGE IN PROGLACIAL AREAS

Basin	Start year	End year	Volumetric change (m ³)		
			Gross deposition	Gross erosion	Net change*
Winthrop	1979	2008	35,000 ± 13,000	2,440,000 ± 53,000 [†]	-2,400,000 ± 57,000 [†]
Winthrop	2008	2017	160,000 ± 30,000	180,000 ± 30,000	-20,000 ± 50,000
Emmons	2005	2008	110,000 ± 25,000	55,000 ± 15,000	60,000 ± 35,000
Emmons	2008	2017	4000 ± 6000	10,000 ± 9000	-6000 ± 19,000
Emmons, not connected to outlet	2008	2017	29,000 ± 10,000	0 ± 2000	30,000 ± 15,000

*Net change is based on unthresholded digital elevation model of difference (DoD) and may not exactly equal gross deposition minus gross erosion.

[†]Minimum estimate; does not include erosion of sediment in areas with glacier ice or vegetation in 1979.

occurred within a set of gully-like channels running along the western margin of the glacier (Fig. 4A). Net erosion from 1979 to 2008, essentially all of which is attributable to the 2006 event, was at least 2,400,000 m³ (Table 2). This volume does not include areas where erosion of sediment was conflated with removal of vegetation or ice, and so it is considered to be a minimum estimate of total sediment erosion.

Sediment entrained in the 2006 storm began to drop out near WF-Vkm 96, just upstream of a narrow bedrock canyon, and 5–10-m-deep deposition continued to the downstream extent of the DoD (WF-Vkm 93). Pervasive young terraces observed in the field in 2017 suggest that substantial valleywide deposition continued for several kilometers beyond this point.

Since 2008, geomorphic activity in the Winthrop proglacial area predominately involved the slumping of eroded gully walls, with material accumulating at the toe of these slopes, accompanied by minor reworking of sediment on the valley floor (Fig. 4B). Net change in the Winthrop proglacial area from 2008 to 2017 was indistinguishable from zero within uncertainty (Table 2).

Downstream of the Winthrop proglacial area, the West Fork White River was predominately erosional over the 2008/2011–2017 period of record (Figs. 4C–4E). Erosion from WF-Vkm 96 to 94 was balanced by deposition between WF-Vkm 93.5 and 91, representing a transfer of material deposited in the 2006 storm from upstream of the bedrock canyon to the valley floor below. Erosion resumed near WF-Vkm 90 and continued over the next 20 km to the confluence with the main-stem White River. Despite locally-complex patterns of storage change, the rate of erosion (m³/km) was relatively consistent when averaged over reaches of several kilometers or more. This is manifest in the roughly linear trend in downstream cumulative net change.

Given the absence of measurable net erosion upstream of WF-Vkm 90 over the 2008–2017 period, net erosion downstream of WF-Vkm 90 appears to have been the dominant source of bed material exiting the basin over this period. That total erosion was 154,000 ± 70,000 m³, equivalent to a mean

bed material export of 26,000 ± 11,500 m³/yr (Table 3; the 2011–2017 interval was used to calculate this average, since nearly all the relevant erosion occurred within the extents of 2011–2017 differencing).

Emmons Proglacial Zone and White River, Park Reach

In contrast to the substantial erosion observed in the Winthrop proglacial area, the 2006 storm caused relatively modest geomorphic change in the Emmons proglacial area, and the change that did occur was predominately depositional (Fig. 5A). The most extensive deposition occurred in a downstream-tapering wedge immediately below the Emmons terminus, with a total volume of 75,000 ± 15,000 m³. Based on the lack of any upstream source area and the alignment with the glacier outlet stream, we believe that this material represents the deposition of subglacially scoured sediment carried by outburst floods of englacially stored water; such outburst floods are well documented in glaciers on Mount Rainier and other regional stratovolcanoes (Driedger and Fountain, 1989; Walder and Driedger, 1994; Slaughter et al., 2004).

From 2008 to 2017, the Emmons proglacial valley floor experienced minor fluvial reworking along the primary glacier outlet stream, erosion and subsequent deposition of material along the glacier-left margin, and the deposition of a small lobe of material along the right margin of the valley (Fig. 5B). Geomorphic changes in these latter two cases were volumetrically minor and do not appear to have delivered material to the primary outlet stream. All told, the low-gradient forefield of the Emmons Glacier appears to have primarily acted as a sink for sediment over the period of record here, with relatively little coarse material exiting the proglacial zone.

After crossing the Emmons proglacial valley floor, the White River cascades down a steep and boulder-studded channel cut through a nineteenth-century terminal moraine and material from a major 1963 rockfall (Crandell and Fahnestock, 1965). At Vkm 105.4, where the river exits back onto a broad gravel braid plain, the valley floor remained unchanged over the 2008–2017 period (Figs. 5B–5F); we take this to

be consistent with relatively little coarse material exiting the upstream proglacial valley over this period. Fluvial activity in the lower braid plain initiated near Vkm 105, where the river undercut a bluff of glacial material on river left; once initiated, geomorphic activity continued down the length of the DoD. Net change was consistently erosional from Vkm 105 to 103; as in the Winthrop, given the lack of detectable net erosion upstream of Vkm 105, erosion of the valley floor downstream of that point appears to have been the dominant source of bed material exported past Vkm 103. That erosion, 30,000 ± 10,000 m³, equates to an annual bed material flux of 3000 ± 1000 m³/yr passing Vkm 103. Downstream of Vkm 103, net deposition from 2008 to 2015 (104,000 ± 79,000 m³) was largely offset by net erosion (-82,000 ± 77,000 m³) from 2015 to 2017, with no detectable net change in storage over the full 2008–2017 period (Table 3; Figs. 5D and 5F).

From 2008 to 2015, net deposition downstream of Vkm 103 exceeded net erosion upstream, implying that the river received bed material from a source not captured in our DoDs (Fig. 5D). Given uncertainty, the volume of this “excess” deposition is not well constrained; regardless, several sediment-rich tributaries or subglacial erosion both provide plausible explanations for the imbalance.

Upper Reach

The upper reach of the White River was nominally net depositional from 2007 to 2011, although the total change did not exceed uncertainty (Fig. 6; Table 3). However, locally significant net deposition or erosion was common over 1–2 km reaches (Figs. 6C and 6D).

Observations from 2011 to 2016 are limited to the lower half of the upper reach, where the White River experienced significant net erosion. This included both erosion of high banks and bluffs and overall lowering of the active channel (Table 3; Figs. 6E, 6F, and 6H). The erosion from banks taller than 2 m accounted for ~100,000 m³, or ~30%, of the total net erosion. This erosion delivered material with an unknown, and potentially fines-dominated, grain size. Considering only erosion of the valley floor and lower

TABLE 3. VOLUMETRIC AND MEAN CHANGE FROM REPEAT TOPOGRAPHIC SURVEYS

Reach	Start year	End year	Upstream valley kilometer	Downstream valley kilometer	Area of analysis (m ²)	Geomorphic change*			Annualized rate of change		
						Net change (m ³)	Mean change (m)	Geomorphic activity† (m ³ /km)	Net change (m ³ /yr)	Mean change (m/yr)	Geomorphic activity rate (m ³ /km/yr)
West Fork White River	2008	2017	97	87	603,600	-27,500 ± 30,000	-0.05 ± 0.05	14,500	-9,000 ± 10,000	-0.005 ± 0.006	1600
West Fork White River	2011	2017	88	70	1,390,000	-154,000 ± 70,000	-0.11 ± 0.05	38,700	-26,000 ± 11,500	-0.018 ± 0.008	6500
Park	2008	2015	107	86	1,584,000	104,000 ± 79,000	0.07 ± 0.05	29,700	15,000 ± 11,000	0.01 ± 0.007	4200
Park	2015	2017	107	86	1,750,000	-82,000 ± 77,000	-0.05 ± 0.05	26,000	-41,000 ± 38,000	-0.03 ± 0.025	13,700
Upper	2007	2011	89	54	3,347,000	107,000 ± 167,000	0.03 ± 0.05	27,000	27,000 ± 42,000	0.01 ± 0.073	6700
Upper	2011	2016	67	51	1,906,000	-308,000 ± 95,000	-0.16 ± 0.05	54,000	-62,000 ± 19,000	-0.03 ± 0.01	10,800
Canyon, upper	2004	2011	33	22	1,981,000	-180,000 ± 99,000	-0.09 ± 0.05	39,000	-26,000 ± 15,000	-0.01 ± 0.007	5600
Canyon, upper	2011	2016	38	22	1,154,000	-9,000 ± 58,000	-0.01 ± 0.05	6000	-19,000 ± 12,000	0.00 ± 0.01	1200
Canyon, lower	2004	2011	21	11	2,720,000	-733,000 ± 136,000	-0.05 ± 0.05	105,000	-19,000 ± 19,000	-0.01 ± 0.007	15,000
Canyon, lower	2011	2016	21	11	2,189,000	-206,000 ± 109,000	-0.09 ± 0.05	39,000	-41,000 ± 22,000	-0.02 ± 0.01	7800
Fan	2004	2011	11	5	453,000	195,000 ± 28,000	0.43 ± 0.05	34,000	28,000 ± 3000	0.06 ± 0.007	4800
Fan	2011	2016	11	5	591,000	219,000 ± 44,000	0.37 ± 0.05	38,000	44,000 ± 6000	0.07 ± 0.01	7500

*Detectable net erosion is shown in blue, while detectable aggradation is shown in red. Change falling within uncertainty bounds is italicized.
 †Geomorphic activity is defined as the absolute sum of gross erosion and gross deposition.

banks, and using the low side of the estimated uncertainty, the loss of storage over this reach implies a conservative minimum downstream bed material flux of 20,000 m³/yr over the 2011–2016 interval.

Sediment Trapping in Mud Mountain Dam

Sediment from the upper reach is passed into the impoundment area of Mud Mountain Dam; although Mud Mountain Dam temporarily traps this sediment when holding a pool, much of that sediment is subsequently flushed through low-elevation outlets between floods. The lack of substantial net sediment accumulation in the impoundment area over the past 80 yr indicates that this flushing is able to pass most of the accumulated suspended silt, sand, and clay (Dunne, 1986). However, there has been no prior analysis focused on the potential trapping of bed material. Here, we documented systematic relations between dam operations and channel conditions, both upstream and downstream of the dam, which suggested that dam operation strategies from 1960 to 1985 tended to promote the trapping of gravel, while changes in those operations since 1985 have allowed a more complete throughput of coarse material; downstream fluxes since 1985 may further have been augmented by erosion of previously trapped sediment (Fig. 7).

The passage of bed material primarily occurs when pool elevations fall below ~279 m, accessing a lower run-of-the-river outlet. From 1960 through 1985, the Mud Mountain Dam pool was typically held above this elevation most of the year (Fig. 7A), creating a small backwater that trapped much of the incoming sand and all of the gravel. The accumulated sediment would then be flushed downstream during planned draw-down periods of several days, typically during low or moderate flows in the summer. Over this 1960–1985 period, valley-floor sediment storage upstream of the dam was generally increasing, while the channel downstream of the dam experienced trends of incision and decreasing or low Froude number, indicating a coarse or armored bed (Figs. 7B–7D). Periods of sediment flushing corresponded to spikes of downstream aggradation, as noted by Dunne (1986), and increased Froude numbers, but these were generally short-lived and the channel tended to return quickly to prior elevations and roughness (Fig. S4; see footnote 1). In combination, we interpret these observations to indicate that flushing events were able to mobilize large volumes of sand out of the dam, temporarily blanketing the downstream channel, but they were neither long enough nor associated with enough shear stress to fully pass accumulated gravel. Gravel storage in the

impoundment was then generally increasing, while the coarse sediment-starved channel downstream experienced an overall trend of incision and coarsening.

Starting around 1985, the number of days per year in which Mud Mountain Dam was held below 279 m increased markedly (Fig. 7A). This change in operations corresponds to a switch to decreasing sediment storage upstream of the dam and aggradation and increasing Froude numbers downstream of the dam (Figs. 7B–7D). Short spikes of aggradation at the downstream gage, previously associated with flushing events, ceased and were replaced by more persistent channel adjustments. We interpret these changes as indicating that the increased time and energy available to pass coarse sediment reestablished a relatively efficient throughput of coarse material. Further, observed negative storage trends through the dam impoundment area since the mid-1980s (Fig. 7B; Fig. S3B) indicate that the impoundment reach has been a net source of sediment, such that bed material fluxes passing Mud Mountain Dam since 1985 have likely been elevated above the natural rate of upstream delivery.

The general trend of aggradation at the gage downstream of the dam ended in 2007 with abrupt incision, as accumulated sediment was flushed further downstream. Channel elevation has since fluctuated around 0.5 m of variability (Fig. 7C). Given that the confined reach around the gage is unlikely to be a long-term site of sediment storage (Fig. S3A), fluctuations since 2007 are interpreted as the transient oscillations of a reach where the delivery of water and sediment has been desynchronized by Mud Mountain Dam operations.

Canyon and Fan Reaches

The canyon reach, linking Mud Mountain Dam to the aggrading fan reach, was net erosional over both the 2004–2011 and 2011–2016 time periods (Fig. 8). Erosion from 2004 to 2011 occurred in three distinct reaches; the first, upstream of Vkm 36, represents the remobilization of gravel delivered from Mud Mountain Dam, as independently observed in the gage analysis (Fig. 7C). The second, starting at Vkm 34, corresponds to a reach noted to be incising after the removal of a grade-control structure in 2003 (Herrera Environmental Consultants, 2010, p. 10). The third and most volumetrically significant erosional reach extends from Vkm 17 to the start of the fan reach at Vkm 12.

From 2011 to 2016, there was little geomorphic activity from Vkm 33 (the upstream extent of the DoD) to Vkm 22. The river was

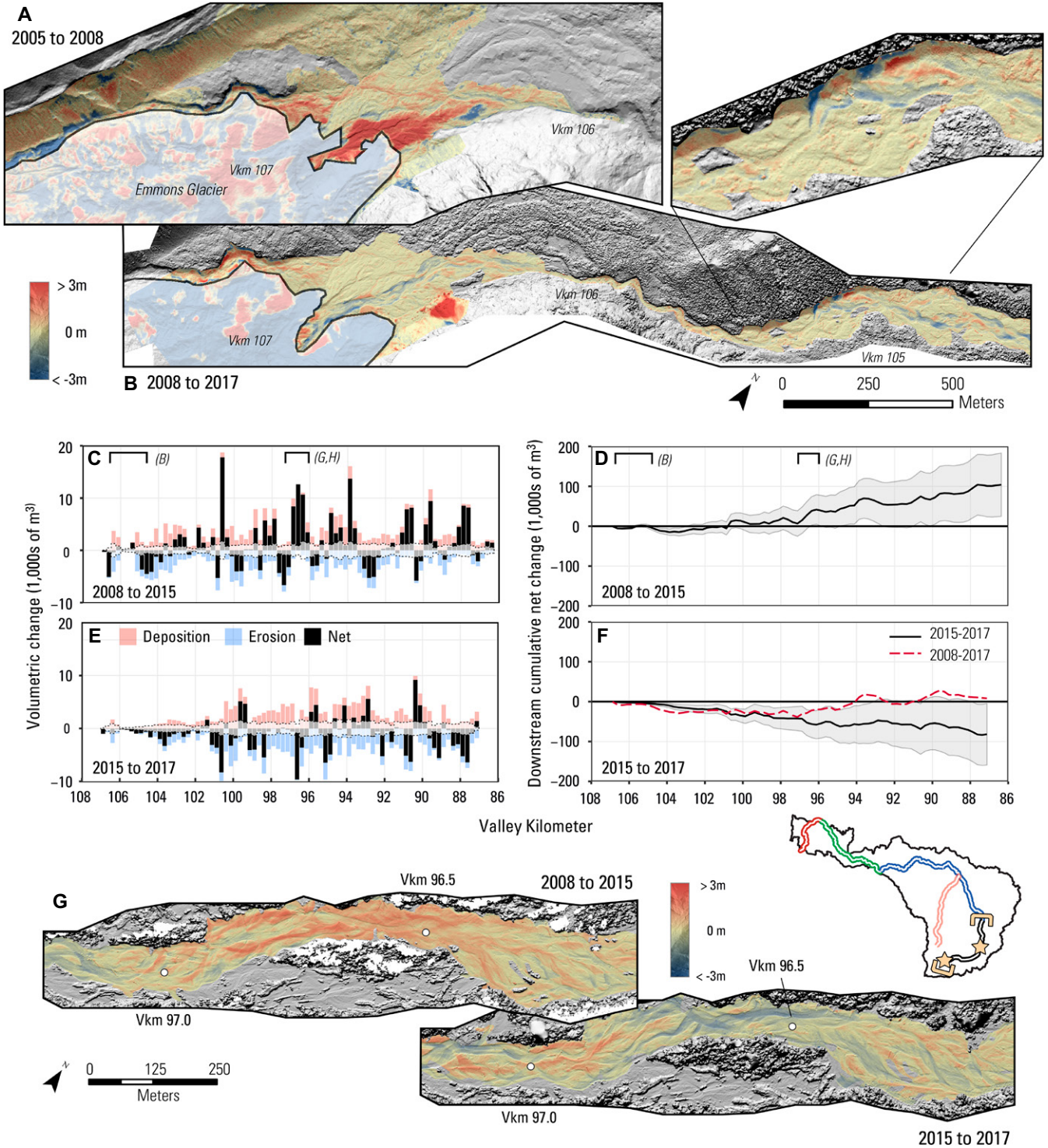


Figure 5. Topographic change in the Emmons proglacial area and park reach of the White River. (A–) Digital elevation model (DEM) of difference showing elevation change in the Emmons proglacial area and uppermost park reach of the White River from 2005 to 2008 (A) and from 2008 to 2017 (B). Shaded areas indicate extent of the Emmons Glacier. Inset highlights onset of geomorphic change downstream of the nineteenth-century moraine. (C) Gross deposition, gross erosion, and net change in sequential 250 m swaths of the park reach of White River, 2008–2015. Gray dashed lines indicate 95% limits of detection. (D) Downstream cumulative sum of net change and 95% confidence intervals, 2008–2015. Brackets in C and D indicate extents of topography shown in B, G, and H. (E) Gross deposition, gross erosion, and net change in sequential 250 m swaths of the park reach of White River, 2015–2017 interval. (F) Downstream cumulative sum of net change and 95% confidence intervals, 2015–2017 interval. (G–H) Example DEM of difference in the White River for 2008–2015 (G) and 2015–2017 (H). Inset in upper right shows analysis locations as described in Figure 4 caption. Vkm—valley kilometer.

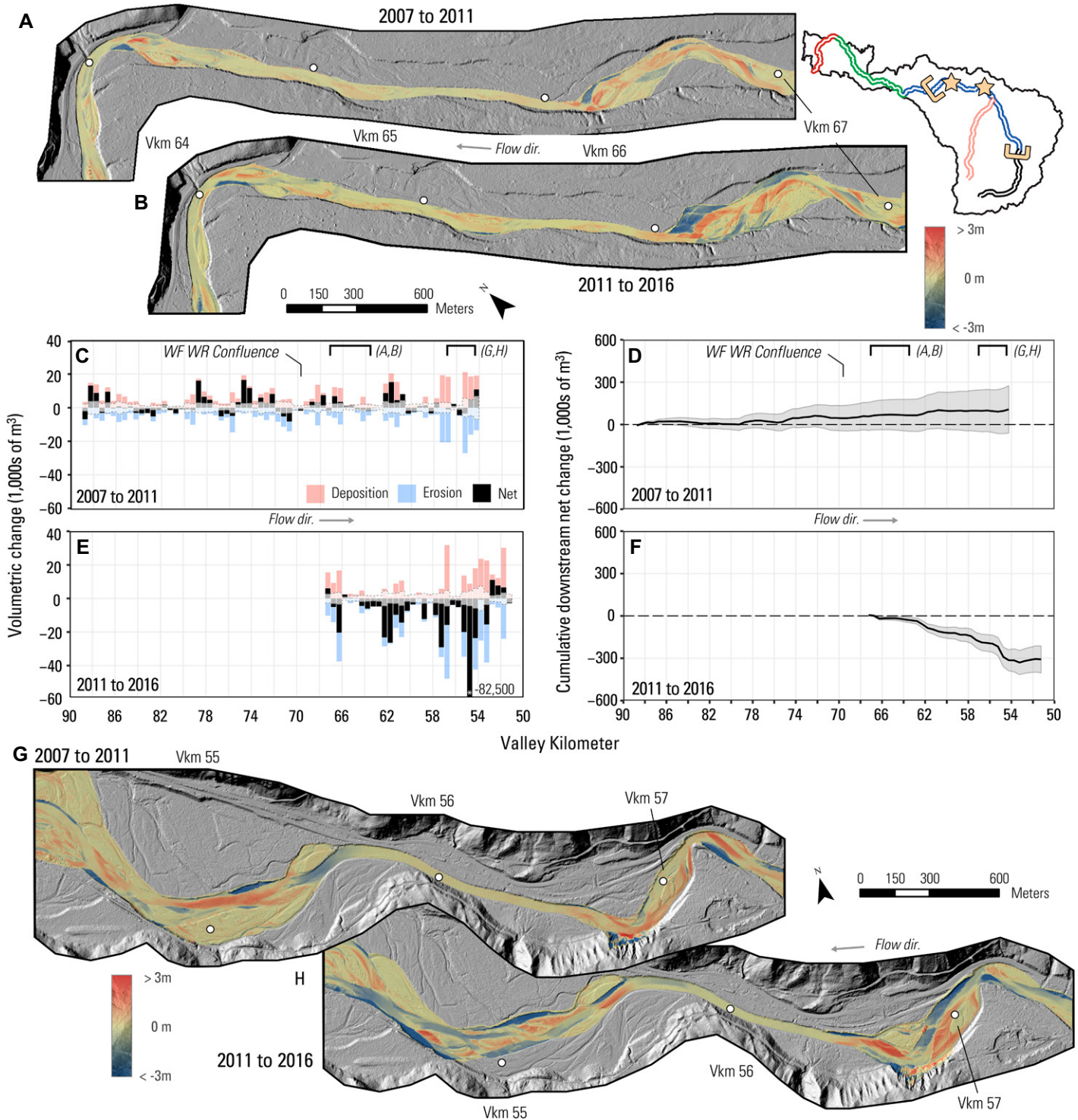


Figure 6. Topographic change in the upper reach of the White River. Figure has same layout as Figure 5, except panels C–F use 500 m valley swaths instead of 250 m swaths. The confluence of the West Fork White River (WF WR) is notated on panels C and D. Vkm—valley kilometer.

then consistently erosional from Vkm 22 to the start of the fan reach. Over both 2004–2011 and 2011–2016 periods, erosion in the canyon reach was primarily associated with erosion of low banks and an overall lowering of the active channel, with relatively minor volumetric con-

tribution from the tall bluffs bounding the reach (Figs. 8A and 8B).

Over both 2004–2011 and 2011–2016, the fan reach experienced pervasive net deposition similar in volume to total net erosion in the canyon reach. Further, over both intervals,

the amount of material eroded from the canyon reach and deposited in the fan reach were similar to the bed-load flux at the boundary of these two reaches, as independently estimated from a measurement-based rating curve (Figs. 8D and 8F; Czuba et al., 2012a). Coupled with

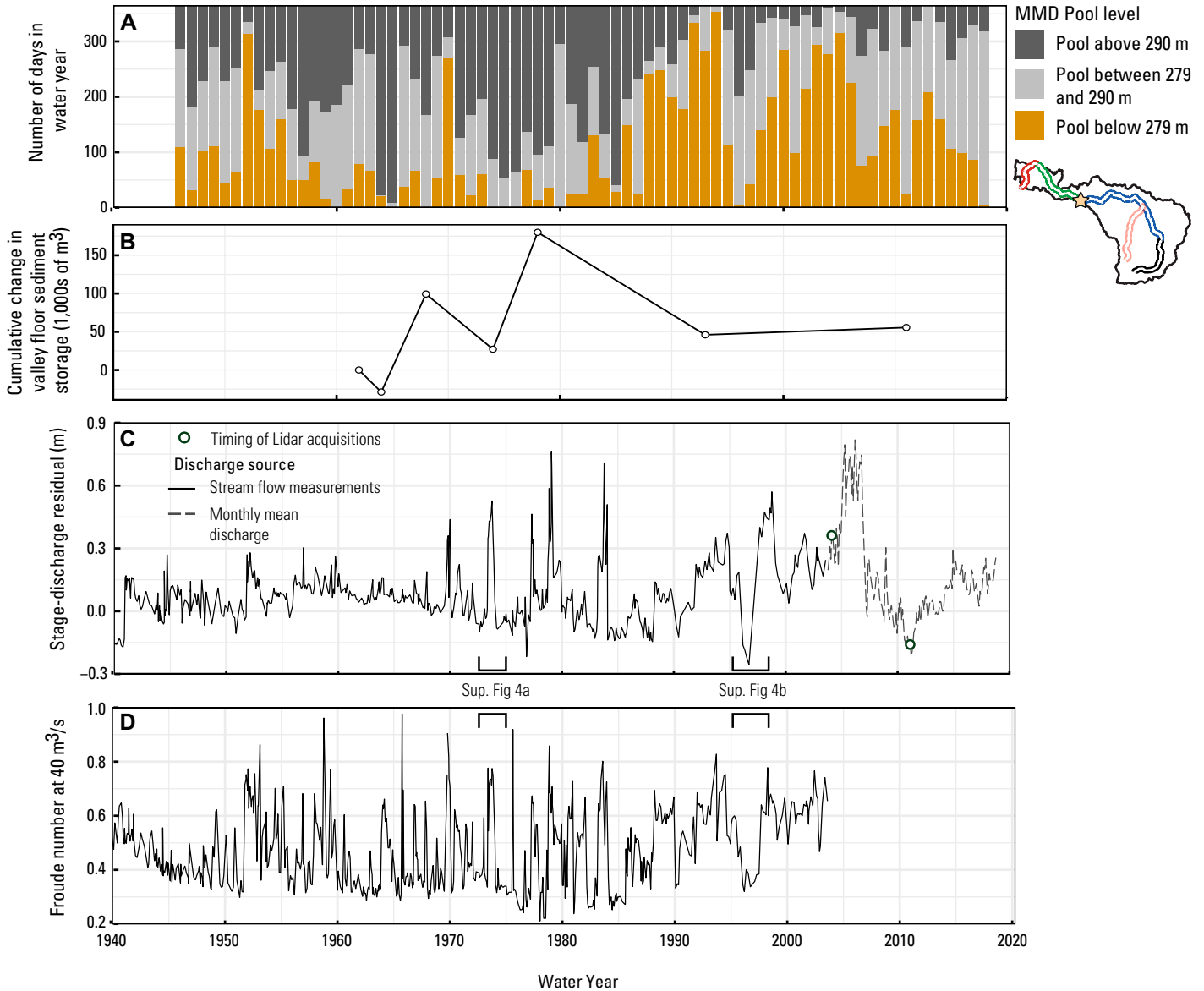


Figure 7. Pool elevations in Mud Mountain Dam (MMD) and channel change in downstream gage. (A) Proportion of water year in which the Mud Mountain Dam impoundment was held at various elevations. A pool below 279 m corresponds to run-of-the-river conditions and allows the passage of coarse sediment. (B) Cumulative sediment storage change in the active channel and low adjacent surfaces through the Mud Mountain Dam impoundment area; analysis only covers lower half of impoundment area (Fig. S3; see text footnote 1). (C) Stage-discharge residuals at U.S. Geological Survey (USGS) gage 12098500, located 2 km downstream of the Mud Mountain Dam outlet (Fig. S3). Residuals at the time of the 2004 and 2011 light detection and ranging (LiDAR) acquisitions are indicated. (D) Froude number, normalized to a common discharge of $40 \text{ m}^3/\text{s}$. Brackets in C and D indicate timing of records shown in Figure S4 (see text footnote 1).

the expectation that gravel flux out the downstream end of the fan reach is essentially zero, these results present a relatively complete and closed bed material budget; sediment deposited in the fan reach has been almost entirely sourced from net erosion of the canyon reach, with relatively little bed material flux entering from upstream or exiting downstream. Given the uncertainty in the elements of this local sediment budget, and the fact that ~20% of total erosion from 2004 to 2011 represented

the remobilization of material recently passed through Mud Mountain Dam and so a delayed delivery of material from upstream, we do not believe that the upstream flux is truly zero. However, these results do imply that net erosion of the lower canyon reach was a consistent and substantial source of the coarse sediment accumulated in the fan reach over the 2004–2016 period of record.

Evidence in the landscape suggests that recent incision in the lower canyon reach is

part of a longer trend. Most notably, channel braid patterns seen in 1940s aerial photography remain clearly visible in 2016 LiDAR data but now sit perched ~4 m above the contemporary channel, indicating a substantial net incision over the past 75 yr (Fig. 9). The presence of a long-term incisional trend is corroborated by repeat cross sections extending back to the 1970s (Czuba et al., 2010; Herrera Environmental Consultants, 2010), which show relatively consistent incision in

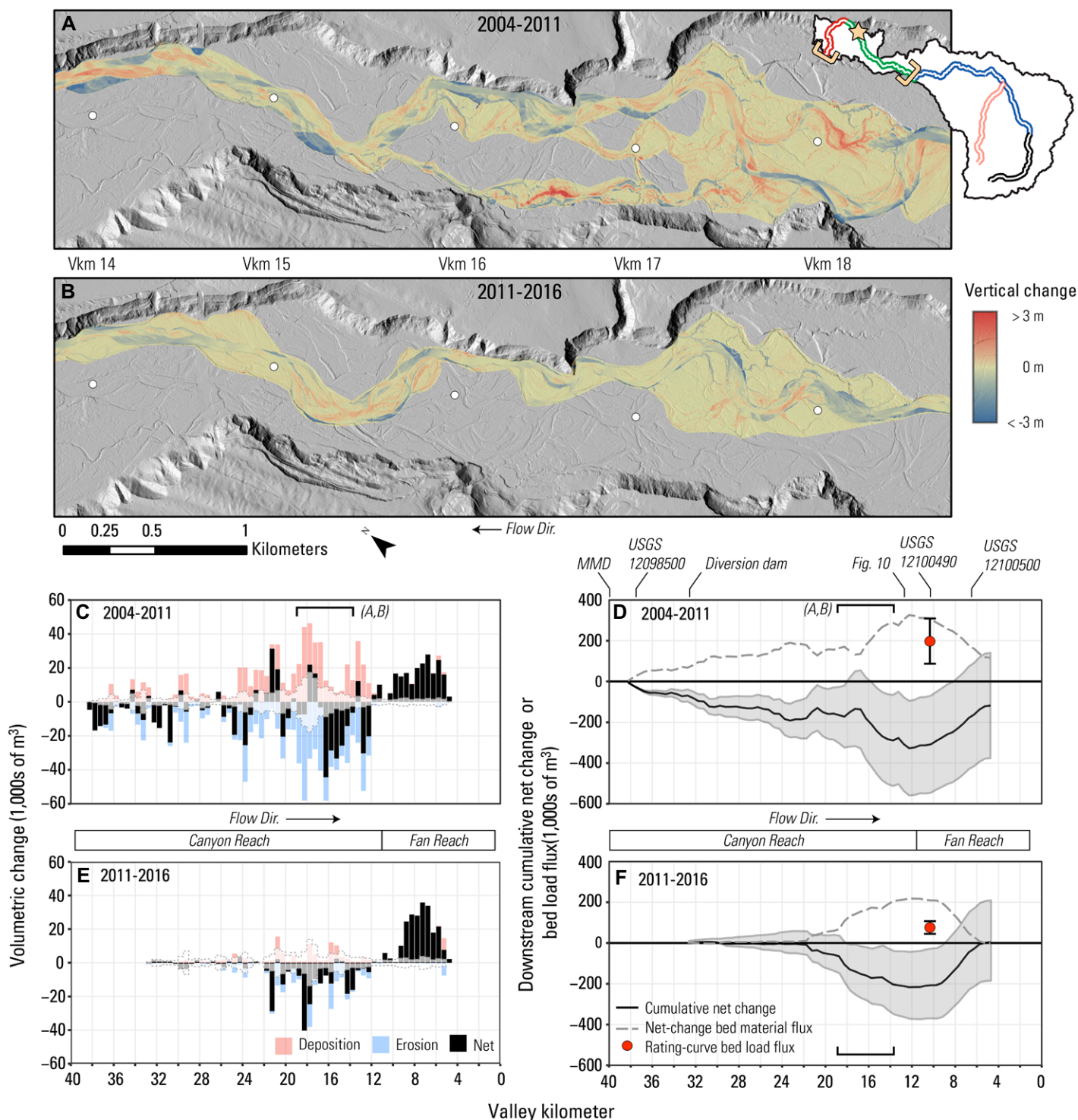


Figure 8. Topographic change in the canyon and fan reaches of the White River. Figure layout is the same as Figures 4–6. Dashed lines in panels D and F are morphologically estimated bed material fluxes, using an upstream boundary condition of zero sediment flux. Uncertainty in the morphologic flux estimate is identical to uncertainty around downstream cumulative net change and was omitted for clarity. Red points are bed-load fluxes estimated from the measurement-based bed-load rating curve of Czuba et al. (2012b) at U.S. Geological Survey (USGS) stream gage 12100490. MMD—Mud Mountain Dam; Vkm—valley kilometer.

the lowermost extents of the canyon reach; river engineers from the 1930s documented substantial and persistent erosion in those

same reaches (Herrera Environmental Consultants, 2010). Together, these results suggest that the lower canyon reach has been

incising at least since the 1930s, with a total lowering at its downstream end of at least 4 m.

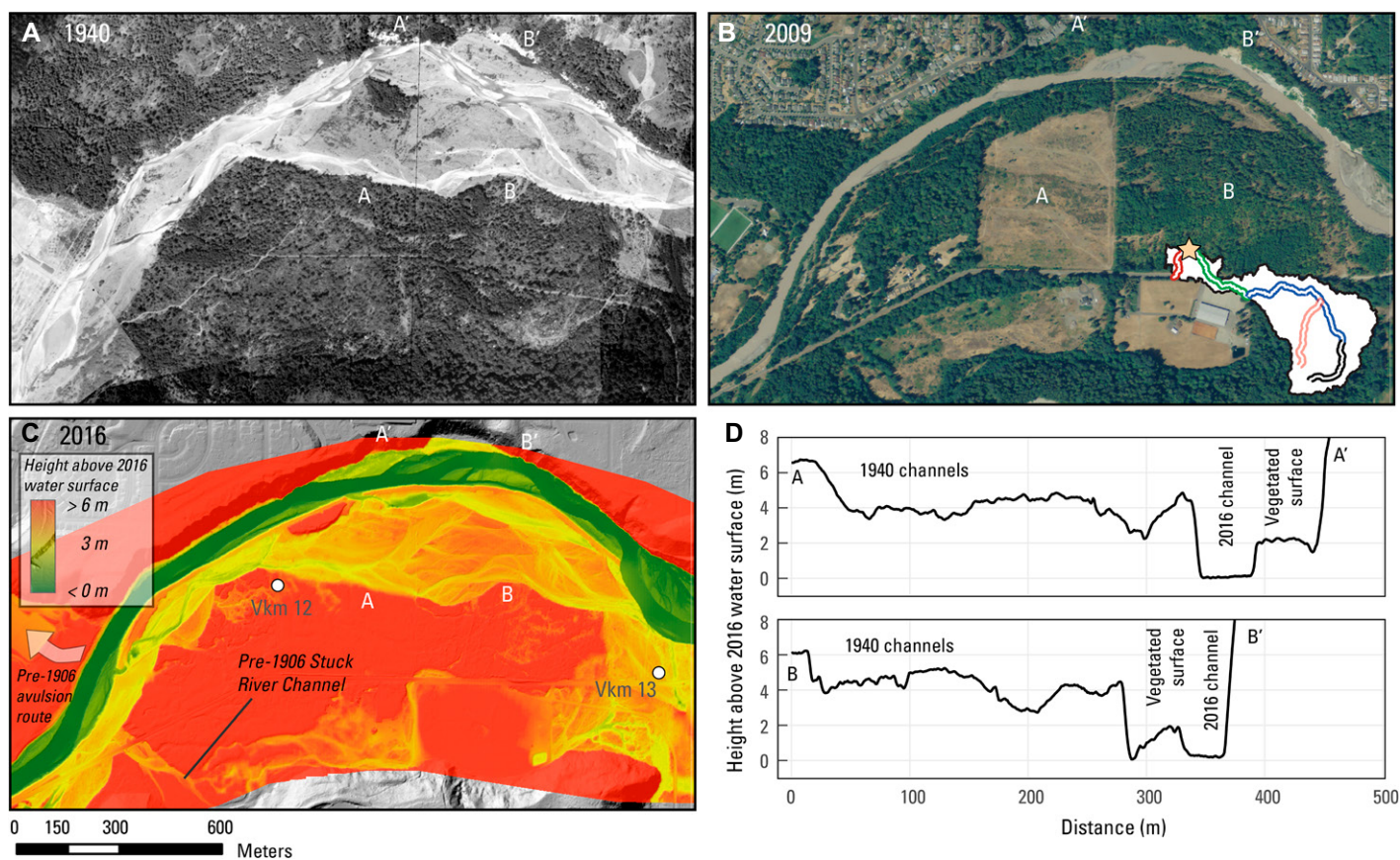


Figure 9. Evidence for incision in the White River immediately upstream of the 1906 avulsion node. (A) Aerial imagery of the White River in 1940. (B) Aerial imagery of the White River in 2009. (C) Height above 2016 water surface, based on 2016 light detection and ranging (LiDAR) data. Active channels present in 1940 imagery are clearly visible in 2016 LiDAR imagery. 1906 avulsion node is at lower left of image; pre-avulsion Stuck River channels run along bottom. (D) Cross sections of the White River valley, plotted as height above 2016 water surface. Locations of cross sections are shown in A–C. Vkm—valley kilometer.

White and Puyallup River Profiles from 1907

Detailed surveys of the lower White, Puyallup, and Duwamish River valleys were completed in 1907, immediately after the 1906 avulsion. Those surveys show that the postavulsion profile of the White River dropped off steeply immediately downstream of the avulsion node (Fig. 10; note this figure plots distance along the 2011 channel centerline (river kilometer, or Rkm) in order to preserve channel slopes; equivalent Vkm distances are given along top axis); the new channel slope was ~40% steeper than either the channel upstream or the abandoned pre-1906 channel course at an equivalent distance downstream. The new channel abruptly flattened near Vkm 8 and remained low gradient until joining with the Puyallup River.

Nearly the entire extents of the lower White and Puyallup Rivers were 2–5 m lower in 2011 than they were in 1907. The one exception is a stretch of the fan reach, centered on Vkm 8, which has filled since 1907. The 2011 profile

has also become more regularly concave than the 1907 profile.

The disjointed 1907 profile of the White River through the Stuck River valley is interpreted as a product of the late Holocene history of river alignments and sediment deposition patterns. After the Osceola Mudflow but before 1906, the majority of the sediment carried by the White River was routed to the north, and the White River fan shows has a distinct northwest alignment and relatively underdeveloped southwest flank (Fig. 10B). Concurrent with the formation of the White River fan, Puyallup River sediment deposits created a broad berm at the southern edge of the Stuck River valley (Fig. 10B). The 1906 avulsion then moved the White River off its reasonably graded, if perched, position along the primary northwest axis of the fan (pre-1906 profile) to the steep, underdeveloped southwest side of the fan (Rkm 10–13 of the 1907 profile) and into the low-gradient backwater of the Stuck River valley (Rkm 0–10). Contrary to the notion that

the White River has likely switched outlets frequently over the late Holocene, this interpretation implies that the 1906 avulsion represents the culmination of filling in the Duwamish Valley to a point where a switch to the south was topographically possible and energetically preferred.

Net lowering of the Puyallup and White Rivers since 1907 can largely be attributed to direct human modification (Herrera Environmental Consultants, 2010). Net incision of the Puyallup River is likely the channel response to significant straightening (Fig. 10B); the magnitude of incision tapers downstream such that the shortened modern channel has reobtained its premodification slope. This incision was largely accomplished by the 1930s, and the lower Puyallup River has been stable or weakly aggrading since that time (Fig. S5; see footnote 1).

Downstream of the avulsion node, much of the lowering of the White River is attributable to dredging, although channelization and the

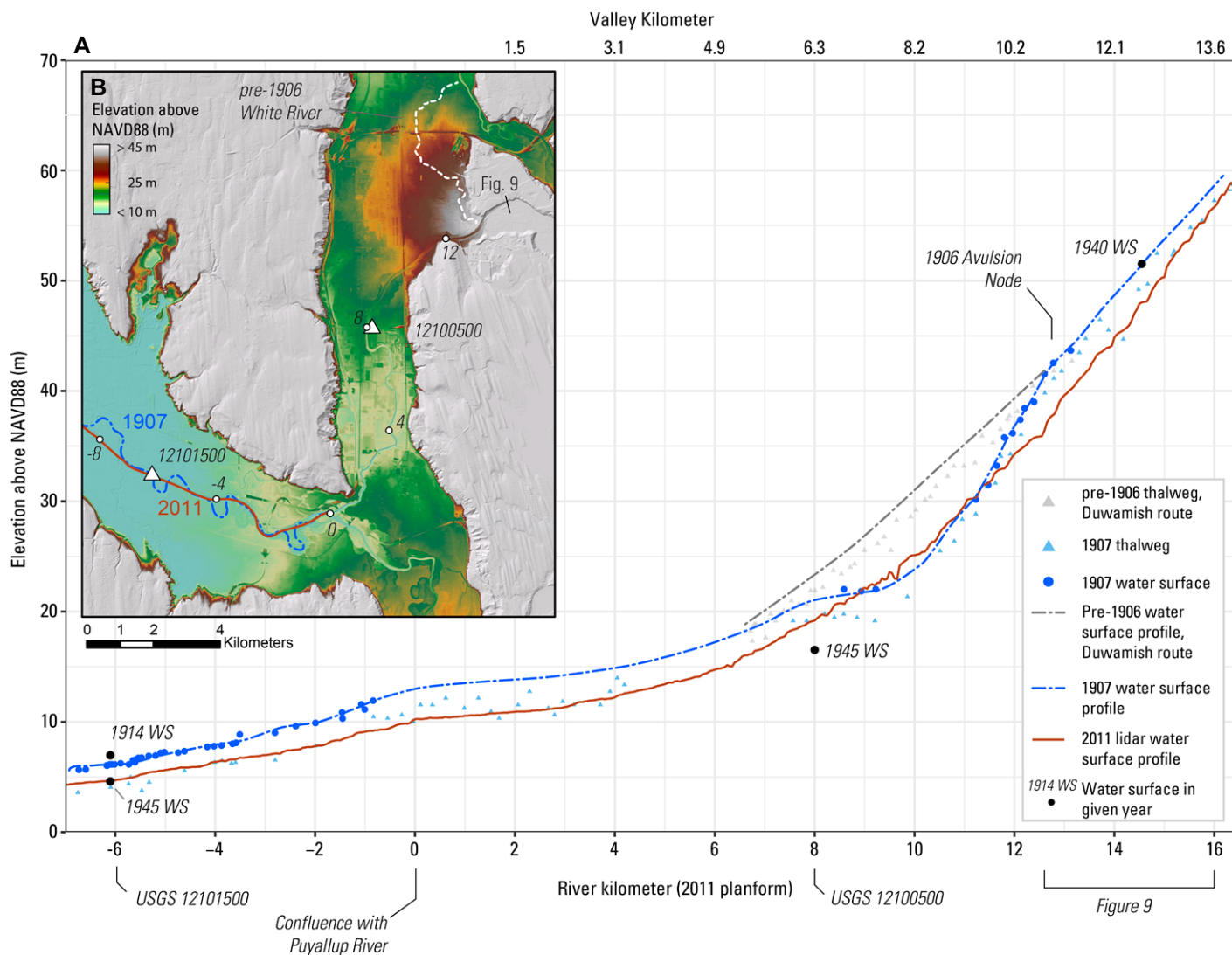


Figure 10. Longitudinal profiles of the fan reach of the White River and Puyallup River based on 1907 channel surveys and 2011 light detection and ranging (LiDAR) data. (A) Water surface (WS) elevation profiles, plotted against distance along the 2011 river centerline. Equivalent distances along the valley centerline used elsewhere in the study are given along top axis. Water surface profiles for 1907 were based on available 1907 water surface and thalweg data points. Water surface elevations at river kilometers –6 and 8 were based on U.S. Geological Survey (USGS) gage data at gages 12101500 (Fig. S5; see text footnote 1) and 12100500 (Fig. 3C), respectively. Water surface elevation at river kilometer 14 was based on elevation of abandoned channels (Fig. 9). (B) Topography of the White River fan, Stuck River valley, and adjacent Puyallup and Duwamish valleys. Planform positions of the Puyallup River in 1907 (blue line) and 2011 (red line) indicate extent of straightening. NAVD88—North American Vertical Datum of 1988.

downstream drop in base level on the Puyallup may have also contributed (Herrera Environmental Consultants, 2010). Gage record near Rkm 8 (Vkm 6) indicate that the channel in 1940 was 4 m lower than in 1907 (Fig. 10A), despite the well-documented tendency for sediment to accumulate in this reach. This provides a rough measure of the amount of net lowering that occurred during early 20th-century dredging.

Upstream of the avulsion node, dredging of the White River has been limited (Herrera Environmental Consultants, 2010). Incision in that

upstream reach is then primarily attributed to the channel response to the drop in downstream base level, initially associated with profile changes during the 1906 avulsion and later augmented by dredging. The persistent incision previously noted in the lower canyon reach over much of the twentieth century (Figs. 8 and 9) is then interpreted as the upstream migration of the knickpoint associated with this change in base level (Begin et al., 1981; Schumm, 1993).

The lower canyon reach is underlain by a downstream-tapering wedge of post-Osceola Mudflow depositional products up to 30 m thick

(Dragovich et al., 1994), implying that a switch from incision to aggradation must have occurred over the post-Osceola period (i.e., the complex response discussed by Schumm and Parker, 1973). Post-1906 incision then represents a rejuvenation of downcutting, and not a continuation or acceleration of persistent late Holocene storage trends.

If the extent of 2011–2016 erosion (Vkm 22) is taken as the upstream extent of that knick zone, the average knickpoint propagation rate would be 110 m/yr over the 110 yr since 1906. The total volume of knickpoint erosion can be roughly

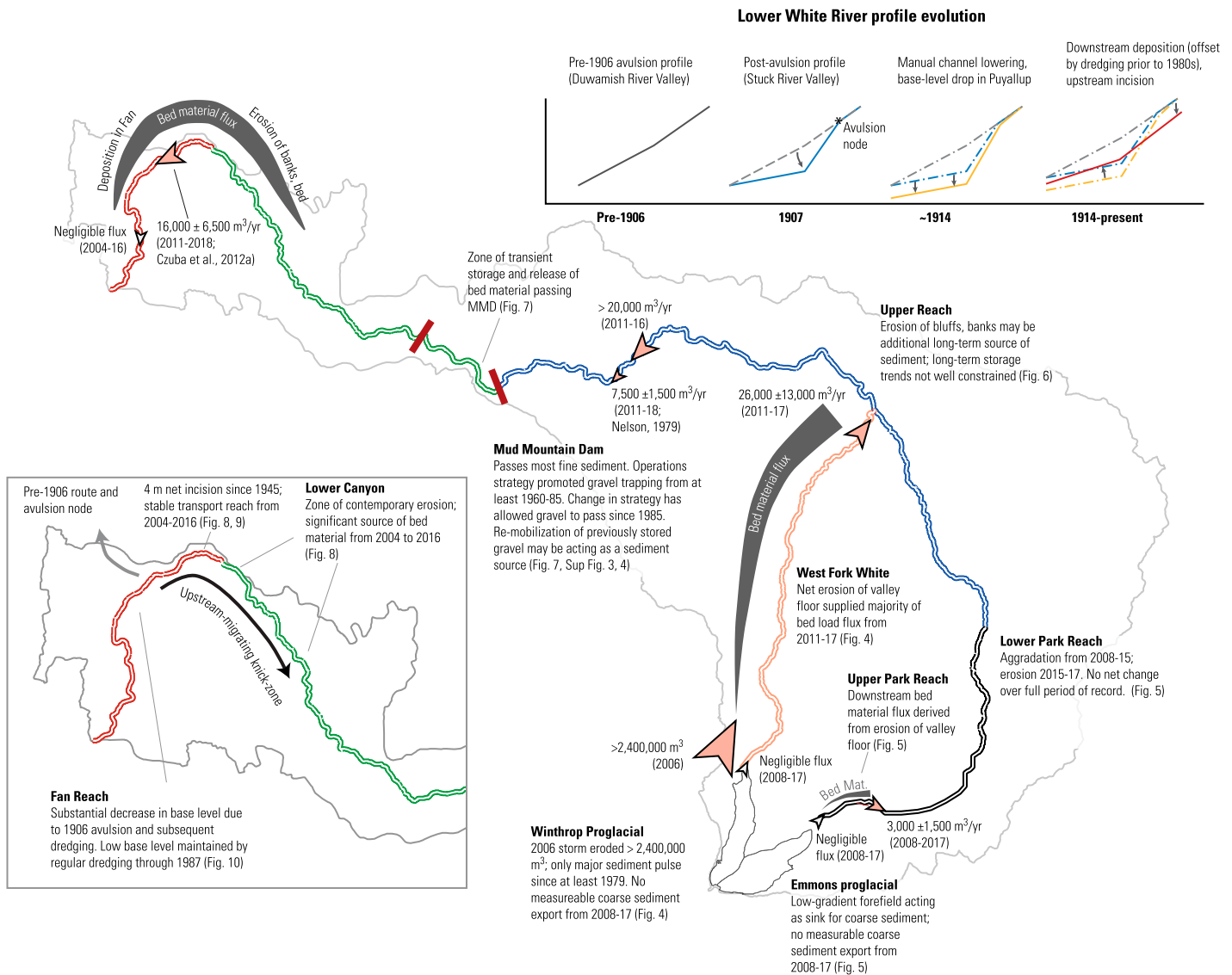


Figure 11. Summary of key findings of bed material delivery and transport in the White River watershed. Locations with estimated bed material or bed-load fluxes are indicated with red arrows; values reflect time periods indicated and may not be representative of long-term means. Reaches with consistent storage trends and associated longitudinal trends in bed material flux over the study period are denoted with gray wedges. Upper-right panel summarizes the sequence of river profile changes in the fan and lower canyon reaches over the historic period. MMD—Mud Mountain Dam.

conceptualized as an upstream-tapering wedge of material, with a downstream thickness of 4 m (Fig. 9) and a planform area of ~2,500,000 m² (the recent active channel area in the lower canyon reach; Table 3); this equates to a total volume of ~5,000,000 m³, equivalent to an average of 45,000 m³/yr from 1907 to 2016. Taking this crude estimate to imply that average knickpoint erosion has likely been on the order of 10,000–100,000 m³/yr, and given recent bed material fluxes of ~16,000 ± 6500 m³/yr, knickpoint-related erosion seems to be sufficiently large to have supplied a large fraction of the total coarse sediment flux reaching the fan over the past century.

DISCUSSION

Integrated Summary of Coarse Sediment Dynamics in the White River

We set out to better understand the contemporary sources and routing of coarse sediment in the White River watershed, motivated by concerns about how short-term climate change may impact coarse sediment fluxes in the lower river. We found that erosion of the lower canyon reach, and not glaciated terrain on Mount Rainier, has been the dominant contemporary source of gravel deposited in the fan reach (Figs. 8 and 11).

Persistent erosion in the lower watershed was further identified as an ongoing river response to a substantial drop in local base level triggered by the 1906 avulsion and augmented by subsequent dredging of the new channel alignment in the early twentieth century (Figs. 9 and 10).

The 1906 avulsion and geometry of the Stuck River valley (Fig. 10) are products of complex river occupation patterns over the late Holocene, as well as the overall conditioning of the lower watershed by continental glaciation. The 1906 valley profile reflects the fact that the pre-1906 Stuck River valley experienced relatively limited sediment delivery over the post-Osceola

Mudflow period, while the (pre-1906) White and Puyallup Rivers continued to fill their own respective valleys. Over the late Holocene, the Stuck River valley then became a low feature in the landscape, bounded by the relatively higher White River fan to the north and Puyallup River deposits to the south. Chronic deposition in the Stuck River valley following the 1906 avulsion reflects the work of the White River to fill and grade that bounded, low valley and build out the relatively less-developed southwest flank of the fan. Recent sediment accumulations in the Stuck River valley are part of the larger process of filling in the Stuck/Duwamish glacial trough, a process substantially accelerated by the rerouting of the White River and the incision of the canyon reach in the aftermath of the Osceola Mudflow. That trough, the sediments eroded out of the canyon reach, and the low drainage divides that allowed outlet-changing avulsions to occur are all products of the sculpting of the Puget Lowlands by continental glaciation.

Although the 1906 avulsion and the valley geometries at that time were essentially natural, the vertical adjustments of the White River following that avulsion have been strongly influenced by human management. Initial dredging of the new course of the White River in the 1910s decreased the already lowered local base level by at least several meters, and continued maintenance dredging through the 1980s prevented that base level from rebounding upwards despite persistent sediment deposition (Fig. 10). Although it is reasonable to presume that the 1906 avulsion alone would have triggered some amount of upstream incision, the artificial lowering and maintenance of the channel profile through the fan reach have likely increased the magnitude and persistence of upstream incision relative to that hypothetical natural trajectory, and so increased the rate and total volume of erosion-related sediment delivery to the fan reach.

Conversely, the construction of a narrow, leved channel through the Stuck River valley has likely increased the throughput of sand and silt that might otherwise have collected in the low-gradient reaches downstream of Vkm 8; Chittenden's survey sheets from 1907 indicate that, prior to construction of that confined channel, this part of the valley was covered in standing water and filling with sand during modest winter flows. The confinement of flow through this low-gradient reach has then likely slowed, or effectively stopped, valley-scale fine sediment deposition across what would have likely been a quasi-deltaic environment.

The importance of the lower canyon reach as a source of bed material implies that the coarse sediment delivery passing through Mud Mountain Dam has been, relatively speaking,

modest. Importantly, this does not appear to be a function of coarse sediment trapping behind Mud Mountain Dam (Fig. 7); over the past several decades, the dam impoundment area has most likely been acting as a transport reach for coarse sediment and, given ongoing erosion in the impoundment area, potentially as a net sediment source (Fig. S3). The modest amount of coarse material passing Mud Mountain Dam is then taken to indicate that the natural delivery to Mud Mountain Dam from the unregulated watershed upstream is similarly modest. This is consistent with crude estimates of bed-load flux based on Nelson's (1979) measurements, which suggest that bed-load delivery to Mud Mountain Dam ($7500 \pm 1500 \text{ m}^3/\text{yr}$) was about half the flux near the fan reach ($16,000 \pm 6500 \text{ m}^3/\text{yr}$) from 2011 to 2018. However, substantial erosion in the lower half of the upper reach implies that the bed material flux at Vkm 50, a few kilometers upstream of Nelson's (1979) sampling site, was at least $20,000 \text{ m}^3/\text{yr}$ from 2011 to 2016 (Fig. 11) and potentially much higher, presenting a somewhat dissonant view of those upstream fluxes.

In the glaciated headwater, the transfer of coarse material from proglacial source areas to downstream river systems was dominated by erosion from the Winthrop Glacier headwaters during the exceptional 2006 storm. No similarly large pulses were observed in the Emmons proglacial area over our period of record, though a well-documented 1963 rockfall (Crandell and Fahnestock, 1964) provides a historical example of such pulses occurring. Outside of the 2006 event in the Winthrop proglacial area, we were unable to detect any substantial coarse sediment export from either basin. Our results then suggest that coarse sediment export from the proglacial areas occurs primarily in episodic pulses with at least multidecadal return intervals. Although the period of record here is somewhat short—38 years for the Winthrop proglacial area and only 12 for the Emmons proglacial area—this inference is consistent with findings in similar alpine headwater settings (i.e., Micheletti and Lane, 2016; Lane et al., 2017).

Over the 2008–2017 period, the primary source of bed material flux carried by the upper White and West Fork White Rivers appears to have been erosion of sediment stored in the valley floor. Over this period, the combined bed material flux from the uppermost White River (Vkm 103) and West Fork White River is then reasonably constrained at $30,000 \pm 11,500 \text{ m}^3/\text{yr}$, with the West Fork White River supplying almost all that total (Fig. 11). However, this average reflects disturbed conditions in the aftermath of the 2006 storm but does not include the presumably large fluxes carried by the 2006 event

itself. It is then unclear how the 2008–2017 export rates compare to longer-term averages.

Ultimately, while the importance of the canyon reach as a source of coarse sediment and the underlying base-level controls on lower-river profile adjustments are supported by multiple lines of evidence, our understanding of the coarse sediment fluxes and dynamics in the full upper watershed remains more limited. In particular, our results place relatively little constraints on the typical bed material fluxes and the presence or absence of any long-term storage trends through the lower park and upper reaches. Coupled with the uncertainty about long-term average rates of sediment export from the upper park and west fork white reaches, and the two somewhat dissonant estimates of bed material fluxes immediately upstream of Mud Mountain Dam, the dynamics linking sediment export from the proglacial river systems to coarse sediment delivery into Mud Mountain Dam remain fuzzy. Improving this understanding and, in particular, obtaining an improved estimate of bed material fluxes entering Mud Mountain Dam would be a useful check on the interpretations presented here. Given the relatively long transport distances of interest and potentially friable volcanic lithologies, understanding the role of attrition will likely be important for a full understanding of the coarse sediment dynamics in the upper watershed and beyond (Attal and Lavé, 2009; O'Connor et al., 2014).

Climate Impacts on Lower-River Sediment Flux and Management of the White River Fan

Over management-relevant time periods of decades, variations in the rate of coarse sediment delivery from headwaters on Mount Rainier, climate-driven or otherwise, seem unlikely to substantially impact the coarse sediment flux near the fan reach. This is most directly because, over these time scales, coarse sediment delivery from the upper watershed makes up only a modest fraction of the total downstream sediment load. Punctuated delivery from proglacial settings may also be strongly modulated by storage dynamics in the upper watershed, with material from large proglacial pulses primarily going into storage to be meted out somewhat more steadily (i.e., Fig. 4).

Although any climate-driven increase in flood activity would presumably tend to increase sediment fluxes through the upper watershed, flood hydrology in the lower watershed is largely dictated by Mud Mountain Dam. Since transport capacity is a non-linear function of discharge, the tendency of the dam to truncate flood peaks, particularly since 2009 (Fig. 3), has likely had a

substantial impact of the integrated shear stress available to erode and transport bed material downstream. Although climate trends would impact the water inflow to Mud Mountain Dam, the operational strategy of that dam is likely to be a larger and more direct control on bed material transport through the Canyon and Fan Reaches.

Ultimately, while forecasted climate trends generally seem more likely to increase coarse sediment transport in the watershed than decrease it, we believe it unlikely that forecasted climate change over the coming decades would result in a substantial increase in coarse sediment delivery to the fan reach. This inferred insensitivity is attributed to the fact that flow regulation, ongoing responses to prior major geomorphic disturbances, and the internal dynamics of storage transfers are, in combination, likely to overprint and/or shred (Jerolmack and Paola, 2010) coarse sediment signals related to short-term climate variability.

We suggest that management concerns in the lower White River may be more geologic than climatic; the underlying disequilibrium of the Stuck River valley implies that aggradation is likely to be a persistent problem for the foreseeable future, regardless of short-term variations in the aggradation rate. Though some of this disequilibrium is attributable to early twentieth-century dredging, and so is limited to the width of the dredged active channel, the entire valley floor remains low relative to likely equilibrium conditions. Bed-load transport modeling (fig. 50 in Czuba et al., 2012a) and comparisons of the pre-avulsion and 2011 profiles (Fig. 9) both suggest that much of the fan reach remains 3 to 8 m below a quasi-equilibrium profile, indicating the scale of fill that would likely occur under natural conditions.

Recognition of this valley-scale disequilibrium will be important when assessing the cost-effectiveness of efforts to increase floodplain connectivity and reduce confinement, since aggradation may rapidly fill in newly opened accommodation space. This would be particularly relevant if newly accessible low-energy environments began to trap the large volumes of suspended sand and silt that have historically passed the confined fan reach.

White River Dynamics as a Paraglacial Response

The Holocene history of the White River is inherently related to the conditioning of the lower watershed by continental glaciation, and the complex dynamics in the lower White River can reasonably be seen as part of the ongoing paraglacial response of regional rivers (Collins and Montgomery, 2011). More specifically,

dynamics in the lower White River provide an example of Ballantyne's (2002a, 2002b) model of an episodically rejuvenated paraglacial sediment response. The notion of episodically rejuvenated or extended paraglacial response as a result of changing base level has been part of the paraglacial literature back to Ryder's (1971) work on dissected alluvial fans, and extreme storms, climatic change, anthropogenic modification, and volcanic activity have all been identified as potential triggers of rejuvenated paraglacial responses in fluvial systems (Jordan and Slaymaker, 1991; Ballantyne, 2002a). Observations in the White River indicate that major avulsions, and ensuing periods of channel adjustment, provide another mechanism for such rejuvenation.

Such avulsions are not limited to the White River; similar events have occurred in many of the major rivers draining through the Puget Lowlands (Ford, 1959; Pittman et al., 2003), and drainage divides between major rivers low enough to be crossed during floods continue to cause problems in the region today. The subtle drainage divides that make these basin-reorganizing avulsions possible are a product of the low-relief landscapes left in the wake of the retreat of continental glaciers; while Ballantyne (2002a) presented paraglacial rejuvenation as a product of primarily extrinsic factors, these avulsions can reasonably be considered as an intrinsic element of the regional paraglacial response. In this sense, these avulsions are similar to river piracy events associated with glacier retreat (i.e., Shugar et al., 2017); both result in substantial modifications to the water and sediment fluxes across multiple basins, both may occur as part of relatively steady processes (glacier retreat or fluvial reworking of glacial sediment) unrelated to external forcing, and both are ultimately a product of the unstable nature of the fluvial network left in the wake of landscape-scale glacier retreat.

The impoundment of trunk streams by paraglacial alluvial fans provides another mechanism for introducing complexity in a paraglacial response, as sediment export out of the trunk stream becomes governed by the interplay between fan growth or decay and the modification of that fan by the trunk stream itself (Fath et al., 2018; Brardinoni et al., 2018). While mechanistically distinct, these dynamics are again intrinsic to the paraglacial response, arising out of the complex interaction between landscape elements.

The consideration of these dynamics suggests that, while the conceptual model of a relatively smooth paraglacial response appears to work well for higher-order streams feeding alluvial fans (i.e., Brardinoni et al., 2018), periodic rejuvenations (or drops) in sediment delivery may be inherent to the paraglacial response of larger watersheds like

the White River, arising purely as a result of the internal complexity in the sediment cascade and the presence of stochastic and/or threshold-dependent processes. This dovetails with the increasing appreciation of autogenic processes in modulating sediment delivery to deposition centers (i.e., Paola, 2016). Given that paraglacial condition still define large swathes of the globe, and that stores of glacial and paraglacial sediment are likely to persist through the duration of the current interglacial period (Brardinoni and Hassan, 2006), we echo Shugar et al. (2018) and Fath et al. (2018) in noting that paraglacial conditioning may result in complex and potentially abrupt shifts in water or sediment fluxes at the watershed scale; recognizing where such threshold-type events have occurred, or may occur, will be important of understanding current landscape states as well as the potential for future change.

While the underlying landscape of the lower White River was formed through continental glaciation, volcanic processes on Mount Rainier have obviously had first-order impacts on the river over the postglacial period. This places the White River within the body of literature related to paraglacial landscapes impacted by Quaternary volcanism, a relatively common overlap along the western margin of North America (Jordan and Slaymaker, 1991; Friele and Clague, 2009). Although Friele and Clague (2009) differentiated the southern Cascade stratovolcanoes, which includes Mount Rainier, from those farther north based on the higher degree of ice-contact volcanism in the latter, the episodic massive pulses of volcanic sediment and generally high rates of Holocene sediment delivery that they discuss seem readily applicable to Mount Rainier and the White River.

Contemporary Proglacial Sediment Dynamics

Concerns about changing sediment delivery from proglacial areas on Mount Rainier have generally been grounded in the concept of a paraglacial response, although this is compounded by potential changes in rainfall frequency/intensity. Although our period of record is too short to directly observe such trends in sediment export, the dynamics we did observe suggest that, over decadal time scales, relationships between proglacial coarse sediment export and climate or glacier extent on Mount Rainier are unlikely to be simple or consistent. This arises for two reasons. First, persistent deposition in the Emmons proglacial area underscores that, while glacier retreat may expose unconsolidated sediment, that same retreat may also open low-gradient extents of the valley floor that trap sediment delivered from further up valley. As has been

widely recognized elsewhere, the timing and magnitude of the sediment response to glacier retreat will depend on the geometry and connectivity of the newly exposed landscape (i.e., Tunnicliffe and Church, 2011; Cavalli et al., 2013; Hoffmann et al., 2013; Messenzehl et al., 2014).

Second, coarse sediment export appears to be dominated by infrequent large pulses, with relatively little export occurring during typical years. This implies that thresholds for motion are relatively high, and that coarse sediment export is then likely to be stochastic over decadal time scales. While changes in climate or glacier extent may influence the underlying probability of large pulses occurring, individual basins may exhibit substantial variability simply due to the random nature of those rare events. Systematic responses to climate or glacier change may then only become apparent when integrated over long time scales or across large spatial scales.

Ultimately, our observations are consistent with prior studies stressing that, while glacier retreat may increase the exposure of mobile sediment, landscape connectivity and often-high thresholds of motion are first-order controls on how that exposed sediment is delivered to downstream river systems, particularly over geologically short time periods (Cavalli et al., 2013; Micheletti and Lane, 2016; Lane et al., 2017; Wohl et al., 2019).

Longitudinally Consistent Erosion Rates

Multiple reaches in the White River watershed experienced consistent rates of storage gain or loss over stretches of many valley kilometers, apparent in the relatively consistent linear trends in plots of downstream cumulative net change. These trends were most apparent in reaches with identifiable disequilibrium conditions (West Fork White River, lower canyon, fan reaches; Figs. 4 and 7), but they appeared throughout the study area. Assuming that geomorphic change down each of these segments involved exchanges of a bed material with similar grain-size distributions, these trends imply that bed material fluxes were steadily increasing or decreasing along the lengths of these same reaches. Similar longitudinally consistent rates of storage gain or loss have been observed in other topographic differencing studies of high-energy transport systems (Anderson and Pitlick, 2014; Gartner et al., 2015; Sholtes et al., 2018), suggesting that these observations are not unique to the White River. Although uniform systematic errors in DoDs can create similar longitudinal consistency, the magnitudes of measured change and good correspondence between measured change and expectations from watershed context or estimated stream power argue against that explanation in the cited studies.

While bed-load or bed material fluxes are often conceptualized as progressively accumulating from tributary sources, these observations highlight that storage dynamics may have as large, if not larger, control on spatial variations in bed-load or bed material fluxes over multi-decadal timescales, such that fluxes may vary substantially (here, by essentially 100%) along relatively homogeneous valley reaches. The fact that the rate of storage gain or loss (or, equivalently, rates of bed material flux increase or decrease) tended to be steady over long reaches is intriguing, as it suggests the possibility of an energetic constraint on the spatial rate of change in the flux; however, more corroborating observations would be needed before this result was considered anything more than a local curiosity or a visual artifact of the smoothing associated with cumulatively summed values.

Landscape History, Storage Dynamics, and River Sensitivity to Disturbance

Cutting across the varied dynamics we observed in the White River, there are two common themes: the central role of sediment storage and the conditioning of contemporary river form and process by past disturbance. In the White River, these two themes are often intertwined; much of the bed material flux carried by annual floods appears to be derived from erosion of existing valley-floor storage, while the original emplacement of valley-scale sediment deposits and the locations of persistent storage gains or losses are often a function of the major geomorphic events over the past 10^2 – 10^4 yr. Specifically, the introduction of bed material into the fluvial system appears to be dominated by glacial processes or infrequent volcanic events and extreme storms, while the spatial patterns of storage redistribution are dictated by both the resulting geometry of those deposits as well as episodic changes in base level. Contemporary patterns of channel change and sediment flux are then largely functions of landscape history, independent of (nonextreme) contemporaneous headwater processes or the detailed sequencing of floods. This does not imply that the current state of the White River was predictable or foreordained, as many of the relevant geomorphic events are inherently stochastic, both in terms of their occurrence and their outcomes.

These themes are by no means novel; the intertwined roles of landscape history and sediment storage are the essence of a paraglacial response (Church and Slaymaker, 1989), and our observations in the White River add to the large body of research highlighting the observations that, in both paraglacial and non-parag-

glacial landscapes, storage exchanges are often central to understanding how sediment is moved through watersheds over periods of years to millennia (i.e., Graf, 1987; Trimble, 1999; Fryirs and Brierley, 2001; Pizzuto et al., 2017; Sutfin and Wohl, 2019) and that the trajectories of storage exchange are often related to extreme or extrafluvial events in the watershed history (i.e., Church and Slaymaker, 1989; Walter and Merritts, 2008; Madej and Ozaki, 2009; James, 2010; Milan, 2012; Joyce et al., 2018; Tunnicliffe et al., 2018).

In the White River, the sequence of watershed disturbances over the Holocene explains much of the contemporary river dynamics and, by extension, strongly influence if and how the river is likely to respond to future disturbance. That landscape history is necessarily unique to the White River, but this uniqueness is, in a sense, common; as has been eloquently argued elsewhere (Simpson, 1963; Schumm, 1991; Lane and Richards, 1998; Phillips, 2007; Church, 2013; Brierley et al., 2013; Phillips, 2017), landscapes are necessarily contingent on past and place. While physics applies everywhere and commonalities will undoubtedly arise, history and contingency are still likely to result in disparate watershed states, and so disparate sensitivities to disturbance, across nominally similar systems. We then reiterate that understanding local geologic, geomorphic, and historic frameworks, encompassing natural and human watershed disturbances and persistent storage trends over $>10^2$ yr time scales, will often be central to understanding how rivers and watersheds are likely to respond to disturbance (Walter and Merritts, 2008; Fryirs, 2013; Pizzuto et al., 2017; Collins et al., 2019; Wohl, 2019).

The ever-growing utilization of repeat high-resolution topography, particularly over long reach to watershed scales, seems a natural tool in this context. These datasets provide measures of both river state and prior change from patch to valley scales within a single consistent framework, and are naturally suited to quantifying storage trends and assessing the impact of contemporary extreme events. This ability to link form and change across a wide range of spatial scales, and particularly for high-intensity events, provides a natural bridge for better understanding how local grain-size and hydraulic processes integrate into valley-scale patterns of storage exchange, or, inversely, how valley-scale storage trends manifest in reach-scale form and function.

CONCLUSION

We set out to better understand the contemporary delivery and routing of coarse sediment in the White River, a large glaciated watershed.

This work was motivated by concerns about the potential for short-term changes in climate to impact coarse sediment delivery to an alluvial fan in the lower watershed. Our results point to persistent erosion of valley floor deposits in the lower watershed as the primary source of bed material deposited in the fan over the past century. Erosion in the lower Canyon Reach and deposition in the Fan Reach were further identified as on-going channel profile adjustments triggered by a major 1906 avulsion across the White River Fan. While the initial disequilibrium in the post-avulsion river profile is attributable to the watershed history of continental glaciation, a major lahar, and changing river valley occupations over the Holocene, that disequilibrium was augmented by substantial dredging of the Fan Reach over much of the 20th century. Somewhat unexpectedly, our results imply that the unregulated upper watershed provides a relatively small fraction of the contemporary coarse sediment load. We suggest that this landscape template, coupled with flow modification from Mud Mountain Dam, make coarse sediment fluxes in the lower watershed relatively insensitive to short-term climate impacts; ultimately, aggradation in the lower White River seems more a function of geology and human management than climate.

More generally, we find that contemporary coarse sediment dynamics throughout the watershed tend to reflect the impact of extreme or extrafluvial events operating over 10²-10⁴ year timescales. The contemporary expression of these events is typically felt in their influence on valley-scale storage dynamics. Specifically, major watershed events appear to introduce much of the coarse sediment stored in the alluvial system (glaciation, volcanism, or extreme storms) or influence the redistribution of that sediment (here, base-level change related to avulsions). Year-to-year flood events appear to primarily remobilize and redistribute existing stored sediment. Our results underscore that the contemporary state of a given river system, and, by extension, the likely response of that river to a given disturbance, will often be dependent on local and potentially idiosyncratic geographic, geologic, and historic factors intertwined with valley-scale storage dynamics.

ACKNOWLEDGMENTS

This study was completed with help from Fred Lott, Judi Radloff, Zac Corum (U.S. Army Corps of Engineers [USACE] Seattle), and Dan Johnson (USACE Mud Mountain Dam). Brian Collins improved this study immensely by providing scanned copies of the 1907 Chittenden survey sheets. Thanks go to Melissa Foster at Quantum Spatial for helping to acquire extended 2016 light detection and ranging (LiDAR) coverage and for supplying ancillary data for previ-

ous acquisitions. Thanks also go to Taylor Kenyon and Scott Beason at Mount Rainier National Park for helping to provide access and logistics for survey work in the national park. We thank Brad Goldman of Gold-Aero for aiding in the collection of aerial imagery.

REFERENCES CITED

- Anderson, S., 2019, Uncertainty in quantitative analyses of topographic change: Error propagation and the role of thresholding: *Earth Surface Processes and Landforms*, v. 44, no. 5, p. 1015–1033, <https://doi.org/10.1002/esp.4551>.
- Anderson, S.W., and Jaeger, K.L., 2019, Supporting Data for Sediment Studies in the White River Watershed: U.S. Geological Survey Data Release, <https://doi.org/10.5066/P9HT46KB>.
- Anderson, S.W., and Konrad, C.P., 2019, Downstream-propagating channel responses to decadal-scale climate variability in a glaciated river basin: *Journal of Geophysical Research—Earth Surface*, v. 124, no. 4, p. 902–919, <https://doi.org/10.1029/2018JF004734>.
- Anderson, S.W., and Pitlick, J., 2014, Using repeat LiDAR to estimate sediment transport in a steep stream: *Journal of Geophysical Research—Earth Surface*, v. 119, no. 3, p. 621–643, <https://doi.org/10.1002/2013JF002933>.
- Anderson, S.W., Keith, M.K., Magirl, C.S., Wallick, J.R., Mastin, M.C., and Foreman, J.R., 2017, Geomorphic Response of the North Fork Stillaguamish River to the State Route 530 Landslide near Oso, Washington: U.S. Geological Survey Scientific Investigations Report 2017–5055, 85 p., <https://doi.org/10.3133/sir20175055>.
- Attal, M., and Lavé, J., 2009, Pebble abrasion during fluvial transport: Experimental results and implications for the evolution of the sediment load along rivers: *Journal of Geophysical Research—Earth Surface*, v. 114, F04023, <https://doi.org/10.1029/2009JF001328>.
- Ballantyne, C.K., 2002a, A general model of paraglacial landscape response: *The Holocene*, v. 12, no. 3, p. 371–376, <https://doi.org/10.1191/0959683602h1553fa>.
- Ballantyne, C.K., 2002b, Paraglacial geomorphology: *Quaternary Science Reviews*, v. 21, no. 18–19, p. 1935–1937, [https://doi.org/10.1016/S0277-3791\(02\)00005-7](https://doi.org/10.1016/S0277-3791(02)00005-7).
- Begin, Z.E.B., Meyer, D.F., and Schumm, S.A., 1981, Development of longitudinal profiles of alluvial channels in response to base-level lowering: *Earth Surface Processes and Landforms*, v. 6, no. 1, p. 49–68, <https://doi.org/10.1002/esp.3290060106>.
- Bogen, J., Xu, M., and Kennie, P., 2015, The impact of proglacial lakes on downstream sediment delivery in Norway: *Earth Surface Processes and Landforms*, v. 40, no. 7, p. 942–952, <https://doi.org/10.1002/esp.3669>.
- Booth, D.B., Troost, K.G., Clague, J.J., and Waitt, R.B., 2003, The Cordilleran ice sheet: *Developments in Quaternary Sciences*, v. 1, p. 17–43, [https://doi.org/10.1016/S1571-0866\(03\)01002-9](https://doi.org/10.1016/S1571-0866(03)01002-9).
- Brardinoni, F., and Hassan, M.A., 2006, Glacial erosion, evolution of river long profiles, and the organization of process domains in mountain drainage basins of coastal British Columbia: *Journal of Geophysical Research—Earth Surface*, v. 111, F01013, <https://doi.org/10.1029/2005JF000358>.
- Brardinoni, F., Picotti, V., Maraio, S., Bruno, P.P., Cucato, M., Morelli, C., and Mair, V., 2018, Postglacial evolution of a formerly glaciated valley: Reconstructing sediment supply, fan building, and confluence effects at the millennial time scale: *Geological Society of America Bulletin*, v. 130, no. 9–10, p. 1457–1473, <https://doi.org/10.1130/B31924.1>.
- Brierley, G., Fryirs, K., Cullum, C., Tadaki, M., Huang, H.Q., and Blue, B., 2013, Reading the landscape: Integrating the theory and practice of geomorphology to develop place-based understandings of river systems. *Progress in Physical Geography*, v. 37, no. 5, p. 601–621, <https://doi.org/10.1177/0309133313490007>.
- Brunsdon, D., and Thornes, J.B., 1979, Landscape sensitivity and change: *Transactions of the Institute of British Geographers*, v. 4, no. 4, p. 463–484, <https://doi.org/10.2307/622210>.
- Carrivick, J.L., and Heckmann, T., 2017, Short-term geomorphological evolution of proglacial systems: *Geomorphology*, v. 287, p. 3–28, <https://doi.org/10.1016/j.geomorph.2017.01.037>.
- Cavalli, M., Trevisani, S., Comiti, F., and Marchi, L., 2013, Geomorphometric assessment of spatial sediment connectivity in small Alpine catchments: *Geomorphology*, v. 188, p. 31–41, <https://doi.org/10.1016/j.geomorph.2012.05.007>.
- Chittenden, H.M., 1907, Report of an Investigation by a Board of Engineers of the Means of Controlling Floods in the Duwamish-Puyallup Valleys and their Tributaries in the State of Washington: Seattle, Washington, Lowman and Hanford S. and P. Co., 32 p.
- Church, M., 2013, Refocusing geomorphology: Field work in four acts: *Geomorphology*, v. 200, p. 184–192, <http://10.1016/j.geomorph.2013.01.014>.
- Church, M., and Ryder, J.M., 1972, Paraglacial sedimentation: A consideration of fluvial processes conditioned by glaciation: *Geological Society of America Bulletin*, v. 83, no. 10, p. 3059–3072, [https://doi.org/10.1130/0016-7606\(1972\)83\[3059:PSACOF\]2.0.CO;2](https://doi.org/10.1130/0016-7606(1972)83[3059:PSACOF]2.0.CO;2).
- Church, M., and Slaymaker, O., 1989, Disequilibrium of Holocene sediment yield in glaciated British Columbia: *Nature*, v. 337, no. 6206, p. 452, <https://doi.org/10.1038/337452a0>.
- Cleveland, W.S., and Devlin, S.J., 1988, Locally weighted regression: An approach to regression analysis by local fitting: *Journal of the American Statistical Association*, v. 83, no. 403, p. 596–610, <https://doi.org/10.1080/01621459.1988.10478639>.
- Collins, B.D., and Montgomery, D.R., 2011, The legacy of Pleistocene glaciation and the organization of lowland alluvial process domains in the Puget Sound region: *Geomorphology*, v. 126, no. 1–2, p. 174–185, <https://doi.org/10.1016/j.geomorph.2010.11.002>.
- Collins, B.D., Dickerson-Lange, S.E., Schanz, S., and Harrington, S., 2019, Differentiating the effects of logging, river engineering, and hydropower dams on flooding in the Skokomish River, Washington, USA: *Geomorphology*, v. 332, p. 138–156, <https://doi.org/10.1016/j.geomorph.2019.01.021>.
- Cooper, R.H., 1983, Effects of Mud Mountain Dam Regulation on Sediment Movement in the White River: Kent, Washington, Northwest Hydraulic Consultants, Inc., 51 p.
- Crandell, D.R., 1971, Postglacial Lahars from Mount Rainier Volcano, Washington: U.S. Geological Survey Professional Paper 677, 75 p., <https://doi.org/10.3133/pp677>.
- Crandell, D.R., and Fahnestock, R.K., 1965, Rockfalls and Avalanches from Little Tahoma Peak on Mount Rainier, Washington: U.S. Geological Survey Bulletin 1221-A, p. A1–A30.
- Crandell, D.R., and Miller, R.D., 1974, Quaternary Stratigraphy and Extent of Glaciation in the Mount Rainier Region, Washington: U.S. Geological Survey Professional Paper 847, 59 p., <https://doi.org/10.3133/pp847>.
- Czuba, J.A., Czuba, C.R., Magirl, C.S., and Voss, F.D., 2010, Channel-Conveyance Capacity, Channel Change, and Sediment Transport in the Lower Puyallup, White, and Carbon Rivers, Western Washington: U.S. Geological Survey Scientific Investigations Report 2010–5240, 104 p., <https://doi.org/10.3133/sir20105240>.
- Czuba, J.A., Magirl, C.S., Czuba, C.R., Curran, C.A., Johnson, K.H., Olsen, T.D., Kimball, H.K., and Gish, C.C., 2012a, Geomorphic Analysis of the River Response to Sedimentation Downstream of Mount Rainier, Washington: U.S. Geological Survey Open-File Report 2012–1242, 134 p., <https://doi.org/10.3133/ofr20121242>.
- Czuba, J.A., Olsen, T.D., Czuba, C.R., Magirl, C.S., and Gish, C.C., 2012b, Changes in Sediment Volume in Alder Lake, Nisqually River Basin, Washington, 1945–2011: U.S. Geological Survey Open-File Report 2012–1068, 30 p., <https://doi.org/10.3133/ofr20121068>.
- Dick, K.A., 2013, Glacier Change in the North Cascades, Washington: 1900–2009 [Master's thesis]: Portland, Oregon, Portland State University, 97 p.
- Dietrich, W.E., and Dunne, T., 1978, Sediment budget for a small catchment in mountainous terrain: *Zeitschrift für Geomorphologie: Supplementband*, v. 29, p. 191–206.
- Dragovich, J.D., Pringle, P.T., and Walsh, T.J., 1994, Extent and geometry of the mid-Holocene Osceola Mudflow in the Puget Lowland—Implications for Holocene sedimentation and paleogeography: *Washington Geology*, v. 22, no. 3, p. 3–26.

- Driedger, C.L., and Fountain, A.G., 1989, Glacier outburst floods at Mount Rainier, Washington State, USA: *Annals of Glaciology*, v. 13, p. 51–55, <https://doi.org/10.3189/S0260305500007631>.
- Driedger, C.L., and Kennard, P.M., 1986, Ice Volumes on Cascade Volcanoes: Mount Rainier, Mount Hood, Three Sisters, and Mount Shasta: U.S. Geological Survey Professional Paper 1365, 42 p.
- Dunne, T., 1986, Sediment Transport and Sedimentation between RMs 5 and 30 along the White River, Washington: Bellevue, Washington, report prepared for Puget Sound Power and Light Company, 39 p.
- East, A.E., Jenkins, K.J., Happe, P.J., Bountry, J.A., Beechie, T.J., Mastin, M.C., Sankey, J.B., and Randle, T.J., 2017, Channel-planform evolution in four rivers of Olympic National Park, Washington, USA: The roles of physical drivers and trophic cascades: *Earth Surface Processes and Landforms*, v. 42, no. 7, p. 1011–1032, <https://doi.org/10.1002/esp.4048>.
- Exner, F.M., 1925, Über die Wechselwirkung zwischen Wasser und Geschiebe in Flüssen: Sitzungsberichte der Kaiserliche Akademie Wissenschaften in Wien—Mathematisch-Naturwissenschaftliche Klasse Abteilung, v. 2a, no. 134, p. 165–203 [in German].
- Fath, J., Clague, J.J., and Friele, P., 2018, Influence of a large debris flow fan on the late Holocene evolution of Squamish River, southwest British Columbia, Canada: *Canadian Journal of Earth Sciences*, v. 55, no. 4, p. 331–342, <https://doi.org/10.1139/cjes-2017-0150>.
- Ford, A.B., 1959, Geology and Petrology of the Glacier Peak Quadrangle, Northern Cascades, Washington [Ph.D. thesis]: Seattle, Washington, University of Washington, 374 p.
- Frans, C.D., 2015, Implications of Glacier Recession for Water Resources [Ph.D. dissertation]: Seattle, Washington University of Washington, 138 p.
- Friele, P.A., and Clague, J.J., 2009, Paraglacial geomorphology of Quaternary volcanic landscapes in the southern Coast Mountains, British Columbia, *in* Knight, J., and Harrison, S., eds., *Periglacial and Paraglacial Processes and Environments*: Geological Society [London] Special Publication 320, p. 219–233, <https://doi.org/10.1144/SP320.14>.
- Fryirs, K., 2013, (Dis) Connectivity in catchment sediment cascades: A fresh look at the sediment delivery problem: *Earth Surface Processes and Landforms*, v. 38, no. 1, p. 30–46, <https://doi.org/10.1002/esp.3242>.
- Fryirs, K.A., 2017, River sensitivity: A lost foundation concept in fluvial geomorphology: *Earth Surface Processes and Landforms*, v. 42, no. 1, p. 55–70, <https://doi.org/10.1002/esp.3940>.
- Fryirs, K., and Brierley, G.J., 2001, Variability in sediment delivery and storage along river courses in Bega catchment, NSW, Australia: Implications for geomorphic river recovery: *Geomorphology*, v. 38, no. 3–4, p. 237–265, [https://doi.org/10.1016/S0169-555X\(00\)00093-3](https://doi.org/10.1016/S0169-555X(00)00093-3).
- Gartner, J.D., Dade, W.B., Renshaw, C.E., Magilligan, F.J., and Buraas, E.M., 2015, Gradients in stream power influence lateral and downstream sediment flux in floods: *Geology*, v. 43, no. 11, p. 983–986, <https://doi.org/10.1130/G36969.1>.
- Gilroy, E.J., Hirsch, R.M., and Cohn, T.A., 1990, Mean square error of regression-based constituent transport estimates: *Water Resources Research*, v. 26, p. 2069, <https://doi.org/10.1029/WR026i009p2069>.
- Graf, W.L., 1987, Late Holocene sediment storage in canyons of the Colorado Plateau: *Geological Society of America Bulletin*, v. 99, no. 2, p. 261–271, [https://doi.org/10.1130/0016-7606\(1987\)99<261:LHSSIC>2.0.CO;2](https://doi.org/10.1130/0016-7606(1987)99<261:LHSSIC>2.0.CO;2).
- Hamlet, A.F., Elsner, M.M., Mauger, G.S., Lee, S.Y., Tohver, I., and Norheim, R.A., 2013, An overview of the Columbia Basin Climate Change Scenarios Project: Approach, methods, and summary of key results: *Atmosphere-Ocean*, v. 51, no. 4, p. 392–415, <https://doi.org/10.1080/07055900.2013.819555>.
- Heckmann, T., McColl, S., and Morche, D., 2016, Retreating ice: Research in pro-glacial areas matters: *Earth Surface Processes and Landforms*, v. 41, no. 2, p. 271–276, <https://doi.org/10.1002/esp.3858>.
- Herrera Environmental Consultants, 2010, Summary of Sediment Trends, Lower White River—RM 4.44 to RM 10.60: Seattle, Washington, report prepared for King County, 10 February 2010, 66 p.
- Hoffmann, T., Müller, T., Johnson, E.A., and Martin, Y.E., 2013, Postglacial adjustment of steep, low-order drainage basins, Canadian Rocky Mountains: *Journal of Geophysical Research—Earth Surface*, v. 118, no. 4, p. 2568–2584, <https://doi.org/10.1002/2013JF002846>.
- James, L.A., 1991, Incision and morphologic evolution of an alluvial channel recovering from hydraulic mining sediment: *Geological Society of America Bulletin*, v. 103, no. 6, p. 723–736, [https://doi.org/10.1130/0016-7606\(1991\)103<0723:IAEMEO>2.3.CO;2](https://doi.org/10.1130/0016-7606(1991)103<0723:IAEMEO>2.3.CO;2).
- James, L.A., 2010, Secular sediment waves, channel bed waves, and legacy sediment: *Geography Compass*, v. 4, no. 6, p. 576–598, <https://doi.org/10.1111/j.1749-8198.2010.00324.x>.
- James, M.R., and Robson, S., 2014, Mitigating systematic error in topographic models derived from UAV and ground-based image networks: *Earth Surface Processes and Landforms*, v. 39, no. 10, p. 1413–1420, <https://doi.org/10.1002/esp.3609>.
- Jerolmack, D.J., and Paola, C., 2010, Shredding of environmental signals by sediment transport: *Geophysical Research Letters*, v. 37, no. 19, L19401, <https://doi.org/10.1029/2010GL044638>.
- Jordan, P., and Slaymaker, O., 1991, Holocene sediment production in Lillooet River basin, British Columbia: A sediment budget approach: *Géographie Physique et Quaternaire*, v. 45, no. 1, p. 45–57, <https://doi.org/10.7202/032844ar>.
- Joyce, H.M., Hardy, R.J., Warburton, J., and Large, A.R., 2018, Sediment continuity through the upland sediment cascade: Geomorphic response of an upland river to an extreme flood event: *Geomorphology*, v. 317, p. 45–61, <https://doi.org/10.1016/j.geomorph.2018.05.002>.
- Konrad, C.P., and Dettinger, M.D., 2017, Flood runoff in relation to water vapor transport by atmospheric rivers over the western United States, 1949–2015: *Geophysical Research Letters*, v. 44, no. 22, p. 11456–11462, <https://doi.org/10.1002/2017GL075399>.
- Lane, S.N., Richards, K.S., and Chandler, J.H., 1995, Morphological estimation of the time-integrated bed load transport rate: *Water Resources Research*, v. 31, no. 3, p. 761–772, <https://doi.org/10.1029/94WR01726>.
- Lane, S.N., and Richards, K.S., 1997, Linking river channel form and process: time, space and causality revisited. *Earth Surface Processes and Landforms: The Journal of the British Geomorphological Group*, v. 22, no. 3, p. 249–260, [https://doi.org/10.1002/\(SICI\)1096-9837\(199703\)22:3<249::AID-ESP752>3.0.CO;2-7](https://doi.org/10.1002/(SICI)1096-9837(199703)22:3<249::AID-ESP752>3.0.CO;2-7).
- Lane, S.N., Bakker, M., Gabbud, C., Micheletti, N., and Saugy, J.N., 2017, Sediment export, transient landscape response and catchment-scale connectivity following rapid climate warming and Alpine glacier recession: *Geomorphology*, v. 277, p. 210–227, <https://doi.org/10.1016/j.geomorph.2016.02.015>.
- Legg, N.T., Meigs, A.J., Grant, G.E., and Kennard, P., 2014, Debris flow initiation in proglacial gullies on Mount Rainier, Washington: *Geomorphology*, v. 226, p. 249–260, <https://doi.org/10.1016/j.geomorph.2014.08.003>.
- Lisle, T.E., 2008, The evolution of sediment waves influenced by varying transport capacity in heterogeneous rivers, *in* Habersack, H., Piegah, H., and Rinaldi, M., eds., *Gravel-Bed Rivers VI: From Process Understanding to River Restoration*: Amsterdam, Netherlands, Elsevier, p. 213–239, [https://doi.org/10.1016/S0928-2025\(07\)11136-6](https://doi.org/10.1016/S0928-2025(07)11136-6).
- Madej, M.A., and Ozaki, V., 2009, Persistence of effects of high sediment loading in a salmon-bearing river, northern California, *in* James, L.A., Rathburn, S.L., and Whittecar, G.R., eds., *Management and Restoration of Fluvial Systems with Broad Historical Changes and Human Impacts*: Geological Society of America Special Paper 451, p. 43–55, [https://doi.org/10.1130/2009.2451\(03\)](https://doi.org/10.1130/2009.2451(03)).
- Mantua, N.J., and Hare, S.R., 2002, The Pacific Decadal Oscillation: *Journal of Oceanography*, v. 58, no. 1, p. 35–44, <https://doi.org/10.1023/A:1015820616384>.
- Mass, C., Skalenakis, A., and Warner, M., 2011, Extreme precipitation over the west coast of North America: Is there a trend?: *Journal of Hydrometeorology*, v. 12, no. 2, p. 310–318, <https://doi.org/10.1175/2010JHM1341.1>.
- Mastin, M.C., Konrad, C.P., Veilleux, A.G., and Tecca, A.E., 2016, Magnitude, Frequency, and Trends of Floods at Gaged and Ungaged Sites in Washington, Based on Data through Water Year 2014 (ver 1.2, November 2017): U.S. Geological Survey Scientific Investigations Report 2016–5118, 70 p., <https://doi.org/10.3133/sir20165118>.
- Mauger, G.S., Casola, J.H., Morgan, H.A., Strauch, R.L., Jones, B., Curry, B., Busch Isaksen, T.M., Whitley Binder, L., Krosby, M.B., and Snover, A.K., 2015, State of Knowledge: Climate Change in Puget Sound: Seattle, Washington, report prepared for the Puget Sound Partnership and the National Oceanic and Atmospheric Administration, Climate Impacts Group, University of Washington, 309 p., <https://doi.org/10.7915/CIG93777D>.
- Meade, R.H., 1988, Movement and storage of sediment in river systems, *in* Letman, A., and Meybeck, M., eds., *Physical and Chemical Weathering in Geochemical Cycles*: Dordrecht, Netherlands, Kluwer, p. 165–179, https://doi.org/10.1007/978-94-009-3071-1_8.
- Menounos, B., and Clague, J.J., 2008, Reconstructing hydroclimatic events and glacier fluctuations over the past millennium from annually laminated sediments of Cheakamus Lake, southern Coast Mountains, British Columbia, Canada: *Quaternary Science Reviews*, v. 27, no. 7, p. 701–713, <https://doi.org/10.1016/j.quascirev.2008.01.007>.
- Messenzehl, K., Hoffmann, T., and Dikau, R., 2014, Sediment connectivity in the high-alpine valley of Val Mütsch, Swiss National Park—Linking geomorphic field mapping with geomorphometric modelling: *Geomorphology*, v. 221, p. 215–229, <https://doi.org/10.1016/j.geomorph.2014.05.033>.
- Micheletti, N., and Lane, S.N., 2016, Water yield and sediment export in small, partially glaciated Alpine watersheds in a warming climate: *Water Resources Research*, v. 52, no. 6, p. 4924–4943, <https://doi.org/10.1002/2016WR018774>.
- Milan, D.J., 2012, Geomorphic impact and system recovery following an extreme flood in an upland stream: Thinhope Burn, northern England, UK: *Geomorphology*, v. 138, no. 1, p. 319–328, <https://doi.org/10.1016/j.geomorph.2011.09.017>.
- Mullineaux, D.R., 1974, Pumice and Other Pyroclastic Deposits in Mount Rainier National Park, Washington: U.S. Geological Survey Bulletin 1326, 83 p.
- Naylor, L.A., Spencer, T., Lane, S.N., Darby, S.E., Magilligan, F.J., Macklin, M.G., and Möller, I., 2017, Stormy geomorphology: Geomorphic contributions in an age of climate extremes: *Earth Surface Processes and Landforms*, v. 42, no. 1, p. 166–190, <https://doi.org/10.1002/esp.4062>.
- Neiman, P.J., Schick, L.J., Ralph, F.M., Hughes, M., and Wick, G.A., 2011, Flooding in western Washington: The connection to atmospheric rivers: *Journal of Hydrometeorology*, v. 12, no. 6, p. 1337–1358, <https://doi.org/10.1175/2011JHM1358.1>.
- Nelson, L.M., 1979, Sediment Transport by the White River into Mud Mountain Reservoir, Washington, June 1974–June 1976: U.S. Geological Survey Water-Resources Investigations Report 78–133, 26 p.
- Nolan, M., Post, A.S., Hauer, W., Zinck, A., and O’Neel, S., 2017, Photogrammetric Scans of Aerial Photographs of North American Glaciers: Arctic Data Center, <https://doi.org/10.18739/A21R9G>.
- Nuth, C., and Kääb, A., 2011, Co-registration and bias corrections of satellite elevation data sets for quantifying glacier thickness change: *The Cryosphere*, v. 5, no. 1, p. 271–290, <https://doi.org/10.5194/tc-5-271-2011>.
- Nylen, T.H., 2004, Spatial and Temporal Variations of Glaciers (1913–1994) on Mt. Rainier and the Relation with Climate [Master’s thesis]: Portland, Oregon, Portland State University, 114 p.
- Ober, R.H., 1898, Report of Mr. R. B. Ober, Surveyor, *in* Report of Capt. Harry Taylor, Corps of Engineers, in “Survey of Duwamish River and its Tributaries, Washington”: Washington, D.C., Annual Report of the U.S. Army Chief of Engineers, Appendix VV17.
- O’Connor, J.E., and Costa, J.E., 1993, Geologic and hydrologic hazards in glaciated basins in North America

- resulting from 19th and 20th century global warming: *Natural Hazards*, v. 8, p. 121–140, <https://doi.org/10.1007/BF00605437>.
- O'Connor, J.E., Mangano, J.F., Anderson, S.W., Wallick, J.R., Jones, K.L., and Keith, M.K., 2014, Geologic and physiographic controls on bed-material yield, transport, and channel morphology for alluvial and bedrock rivers, western Oregon: *Geological Society of America Bulletin*, v. 126, no. 3–4, p. 377–397, <https://doi.org/10.1130/B30831.1>.
- Paola, C., 2016, A mind of their own: Recent advances in autogenic dynamics in rivers and deltas, in Budd, D.A., Hajek, E.A., and Purkis, S.J., eds., *Autogenic Dynamics and Self-Organization in Sedimentary Systems: Society for Sedimentary Geology (SEPM) Special Publication 106*, p. 5–17, <https://doi.org/10.2110/sepm106.04>.
- Paola, C., and Voller, V.R., 2005, A generalized Exner equation for sediment mass balance: *Journal of Geophysical Research—Earth Surface*, v. 110, F04014, <https://doi.org/10.1029/2004JF000274>.
- Pfeiffer, A.M., Collins, B.D., Anderson, S.W., Montgomery, D.R., and Istanbuluoglu, E., 2019, River bed elevation variability reflects sediment supply, rather than peak flows, in the uplands of Washington State: *Water Resources Research*, v. 55, no. 8, p. 6795–6810, <https://doi.org/10.1029/2019WR025394>.
- Pittman, P., Maudlin, M., and Collins, B., 2003, Evidence of a major late Holocene river avulsion: *Geological Society of America Abstracts with Programs*, v. 35, no. 6, p. 334.
- Pizzuto, J., Keeler, J., Skalak, K., and Karwan, D., 2017, Storage filters upland suspended sediment signals delivered from watersheds: *Geology*, v. 45, no. 2, p. 151–154, <https://doi.org/10.1130/G38170.1>.
- Phillips, J.D., 2007, The perfect landscape: *Geomorphology*, v. 84, no. 3–4, p. 159–169, <https://doi.org/10.1002/esp.4083>.
- Phillips, J.D., 2017, Laws, place, history and the interpretation of landforms: *Earth Surface Processes and Landforms*, v. 42, p. 347–354, <https://doi.org/10.1002/esp.4083>.
- Prych, E.A., 1988, Flood-Carrying Capacities and Changes in Channels of the Lower Puyallup, White, and Carbon Rivers in Western Washington: U.S. Geological Survey Water-Resources Investigation 87–4129, 71 p.
- Reid, M.E., Sisson, T.W., and Brien, D.L., 2001, Volcano collapse promoted by hydrothermal alteration and edifice shape, Mount Rainier, Washington: *Geology*, v. 29, no. 9, p. 779–782, [https://doi.org/10.1130/0091-7613\(2001\)029<0779:VCPBHA>2.0.CO;2](https://doi.org/10.1130/0091-7613(2001)029<0779:VCPBHA>2.0.CO;2).
- Ritchie, A.C., Warrick, J.A., East, A.E., Magirl, C.S., Stevens, A.W., Bountry, J.A., Randle, T.J., Curran, C.A., Hilldale, R.C., Duda, J.J., and Gelfenbaum, G.R., 2018, Morphodynamic evolution following sediment release from the world's largest dam removal: *Scientific Reports*, v. 8, 13279, <https://doi.org/10.1038/s41598-018-30817-8>.
- Rolstad, C., Haug, T., and Denby, B., 2009, Spatially integrated geodetic glacier mass balance and its uncertainty based on geostatistical analysis: Application to the western Svartisen ice cap, Norway: *Journal of Glaciology*, v. 55, no. 192, p. 666–680, <https://doi.org/10.3189/002214309789470950>.
- Ryder, J.M., 1971, The stratigraphy and morphology of paraglacial alluvial fans in south-central British Columbia: *Canadian Journal of Earth Sciences*, v. 8, no. 2, p. 279–298, <https://doi.org/10.1139/e71-027>.
- Salathé, E.P., Jr., Hamlet, A.F., Mass, C.F., Lee, S.Y., Stumbaugh, M., and Steed, R., 2014, Estimates of twenty-first-century flood risk in the Pacific Northwest based on regional climate model simulations: *Journal of Hydrometeorology*, v. 15, no. 5, p. 1881–1899, <https://doi.org/10.1175/JHM-D-13-0137.1>.
- Schumm, S.A., 1991, *To Interpret the Earth: Ten Ways to be Wrong*: New York, Cambridge University Press.
- Schumm, S.A., 1993, River response to base-level change: Implications for sequence stratigraphy: *The Journal of Geology*, v. 101, no. 2, p. 279–294, <https://doi.org/10.1086/648221>.
- Schumm, S.A., and Parker, R.S., 1973, Implications of complex response of drainage systems for Quaternary alluvial stratigraphy: *Nature—Physical Science (London)*, v. 243, no. 128, p. 99–100, <https://doi.org/10.1038/physci243099a0>.
- Sholtes, J.S., Yochum, S.E., Scott, J.A., and Bledsoe, B.P., 2018, Longitudinal variability of geomorphic response to floods: *Earth Surface Processes and Landforms*, v. 43, no. 15, p. 3099–3113, <https://doi.org/10.1002/esp.4472>.
- Shugar, D.H., Clague, J.J., Best, J.L., Schoof, C., Willis, M.J., Copland, L., and Roe, G.H., 2017, River piracy and drainage basin reorganization led by climate-driven glacier retreat: *Nature Geoscience*, v. 10, no. 5, p. 370–375, <https://doi.org/10.1038/ngeo2932>.
- Sikonia, W.G., 1990, Sediment Transport in the Lower Puyallup, White, and Carbon Rivers of Western Washington: U.S. Geological Survey Water-Resources Investigations Report 89–4112, 84 p. (Also available at <http://pubs.er.usgs.gov/publication/wri894112>.)
- Simpson, G.G., 1963, Historical science, in Albritton, C.C., ed., *The Fabric of Geology*: Reading, Addison-Wesley, p. 24–48.
- Simpson, G., and Castellort, S., 2012, Model shows that rivers transmit high-frequency climate cycles to the sedimentary record: *Geology*, v. 40, no. 12, p. 1131–1134, <https://doi.org/10.1130/G33451.1>.
- Slater, L.J., Singer, M.B., and Kirchner, J.W., 2015, Hydrologic versus geomorphic drivers of trends in flood hazard: *Geophysical Research Letters*, v. 42, no. 2, p. 370–376, <https://doi.org/10.1002/2014GL062482>.
- Slaughter, S.L., Ely, L.L., and Scott, K.M., 2004, The 1938 Chocolate Glacier debris flow, Glacier Peak volcano, North Cascades, Washington: *Geological Society of America Abstracts with Programs*, v. 36, no. 4, p. 14.
- Stewart, I.T., 2009, Changes in snowpack and snowmelt runoff for key mountain regions: *Hydrological Processes: An International Journal*, v. 23, no. 1, p. 78–94, <https://doi.org/10.1002/hyp.7128>.
- Stoelinga, M.T., Albright, M.D., and Mass, C.F., 2010, A new look at snowpack trends in the Cascade Mountains: *Journal of Climate*, v. 23, no. 10, p. 2473–2491, <https://doi.org/10.1175/2009JCLI2911.1>.
- Sutfin, N.A., and Wohl, E., 2019, Elevational differences in hydrogeomorphic disturbance regime influence sediment residence times within mountain river corridors: *Nature Communications*, v. 10, no. 1, p. 2221, <https://doi.org/10.1038/s41467-019-09864-w>.
- Tohver, I.M., Hamlet, A.F., and Lee, S.Y., 2014, Impacts of 21st-century climate change on hydrologic extremes in the Pacific Northwest region of North America: *Journal of the American Water Resources Association*, v. 50, no. 6, p. 1461–1476, <https://doi.org/10.1111/jawr.12199>.
- Trimble, S.W., 1997, Contribution of stream channel erosion to sediment yield from an urbanizing watershed: *Science*, v. 278, no. 5342, p. 1442–1444, <https://doi.org/10.1126/science.278.5342.1442>.
- Trimble, S.W., 1999, Decreased rates of alluvial sediment storage in the Coon Creek Basin, Wisconsin, 1975–93: *Science*, v. 285, no. 5431, p. 1244–1246, <https://doi.org/10.1126/science.285.5431.1244>.
- Tunncliffe, J., and Church, M., 2011, Scale variation of post-glacial sediment yield in Chilliwack Valley, British Columbia: *Earth Surface Processes and Landforms*, v. 36, no. 2, p. 229–243, <https://doi.org/10.1002/esp.2093>.
- Tunncliffe, J., Brierley, G., Fuller, I.C., Leenan, A., Marden, M., and Peacock, D., 2018, Reaction and relaxation in a coarse-grained fluvial system following catchment-wide disturbance: *Geomorphology*, v. 307, p. 50–64, <https://doi.org/10.1016/j.geomorph.2017.11.006>.
- Vallance, J.W., and Scott, K.M., 1997, The Osceola Mudflow from Mount Rainier—Sedimentology and hazard implications of a huge clay-rich debris flow: *Geological Society of America Bulletin*, v. 109, no. 2, p. 143–163, [https://doi.org/10.1130/0016-7606\(1997\)109<0143:TOMFMR>2.3.CO;2](https://doi.org/10.1130/0016-7606(1997)109<0143:TOMFMR>2.3.CO;2).
- Walder, J.S., and Driedger, C.L., 1994, Rapid geomorphic change caused by glacial outburst floods and debris flows along Tahomah Creek, Mount Rainier, Washington, U.S.A.: *Arctic and Alpine Research*, v. 26, no. 4, p. 319–327, <https://doi.org/10.2307/1551792>.
- Walling, D.E., 1983, The sediment delivery problem: *Journal of Hydrology (Amsterdam)*, v. 65, p. 209–237, [https://doi.org/10.1016/0022-1694\(83\)90217-2](https://doi.org/10.1016/0022-1694(83)90217-2).
- Walter, R.C., and Merritts, D.J., 2008, Natural streams and the legacy of water-powered mills: *Science*, v. 319, no. 5861, p. 299–304, <https://doi.org/10.1126/science.1151716>.
- Warrick, J.A., 2015, Trend analyses with river sediment rating curves: *Hydrological Processes*, v. 29, no. 6, p. 936–949, <https://doi.org/10.1002/hyp.10198>.
- Warner, M.D., Mass, C.F., and Salathé, E.P., Jr., 2015, Changes in winter atmospheric rivers along the North American west coast in CMIP5 climate models: *Journal of Hydrometeorology*, v. 16, no. 1, p. 118–128, <https://doi.org/10.1175/JHM-D-14-0080.1>.
- Wheaton, J.M., Brasington, J., Darby, S.E., and Sear, D.A., 2010, Accounting for uncertainty in DEMs from repeat topographic surveys: improved sediment budgets, Earth surface processes and landforms: *The Journal of the British Geomorphological Research Group*, v. 35, no. 2, p. 136–156, <https://doi.org/10.1002/esp.1886>.
- Whitfield, P.H., Moore, R.D., Fleming, S.W., and Zawadzki, A., 2010, Pacific Decadal Oscillation and the hydroclimatology of western Canada—Review and prospects: *Canadian Water Resources Journal*, v. 35, no. 1, p. 1–28, <https://doi.org/10.4296/cwrj3501001>.
- Wohl, E., 2019, Forgotten legacies: Understanding and mitigating historical human alterations of river corridors: *Water Resources Research*, v. 55, no. 7, p. 5181–5201, <https://doi.org/10.1029/2018WR024433>.
- Wohl, E., Brierley, G., Cadol, D., Coulthard, T.J., Covino, T., Fryirs, K.A., Grant, G., Hilton, R.G., Lane, S.N., Magilligan, F.J., and Meitzen, K.M., 2019, Connectivity as an emergent property of geomorphic systems: *Earth Surface Processes and Landforms*, v. 44, no. 1, p. 4–26, <https://doi.org/10.1002/esp.4434>.
- Zemp, M., Hoelzle, M., and Haeblerli, W., 2009, Six decades of glacier mass-balance observations: A review of the worldwide monitoring network: *Annals of Glaciology*, v. 50, no. 50, p. 101–111, <https://doi.org/10.3189/172756409787769591>.

SCIENCE EDITOR: BRAD S. SINGER
ASSOCIATE EDITOR: JOHN JANSEN

MANUSCRIPT RECEIVED 15 OCTOBER 2019
REVISED MANUSCRIPT RECEIVED 20 MARCH 2020
MANUSCRIPT ACCEPTED 15 JUNE 2020

Printed in the USA